

Channel Estimation for Diffusive Molecular Communications

Vahid Jamali, *Student Member, IEEE*, Arman Ahmadzadeh, *Student Member, IEEE*, Christophe Jardin, Heinrich Sticht, and Robert Schober, *Fellow, IEEE*

Abstract—In molecular communication (MC) systems, the expected number of molecules observed at the receiver over time after the instantaneous release of molecules by the transmitter is referred to as the channel impulse response (CIR). Knowledge of the CIR is needed for the design of detection and equalization schemes. In this paper, we present a training-based CIR estimation framework for MC systems which aims at estimating the CIR based on the observed number of molecules at the receiver due to emission of a sequence of known numbers of molecules by the transmitter. Thereby, we distinguish two scenarios depending on whether or not statistical channel knowledge is available. In particular, we derive maximum likelihood (ML) and least sum of square errors (LSSE) estimators which do not require any knowledge of the channel statistics. For the case, when statistical channel knowledge is available, the corresponding maximum a posteriori (MAP) and linear minimum mean square error (LMMSE) estimators are provided. As performance bound, we derive the classical Cramer Rao (CR) lower bound, valid for any unbiased estimator, which does not exploit statistical channel knowledge, and the Bayesian CR lower bound, valid for any unbiased estimator, which exploits statistical channel knowledge. Finally, we propose optimal and suboptimal training sequence designs for the considered MC system. Simulation results confirm the analysis and compare the performance of the proposed estimation techniques with the respective CR lower bounds.

Index Terms—Molecular communications, channel impulse response estimation, Cramer Rao lower bound, and training sequence design.

I. INTRODUCTION

Recent advances in biology, nanotechnology, and medicine have enabled the possibility of communication in nano/micrometer scale environments [1]–[3]. Thereby, employing molecules as information carriers, molecular communication (MC) has quickly emerged as a bio-inspired approach for man-made communication systems in such environments. In fact, calcium signaling among neighboring cells, the use of neurotransmitters for communication across the synaptic cleft of neurons, and the exchange of autoinducers as signaling molecules in bacteria for quorum sensing are among the many examples of MC in nature [3], [4].

This paper was presented in part at the International Conference on Communications (ICC) 2016, Kuala Lumpur, Malaysia [31].

V. Jamali, A. Ahmadzadeh, and R. Schober are with the Institute for Digital Communications at the Friedrich-Alexander University (FAU), Erlangen, Germany (email: vahid.jamali@fau.de, arman.ahmadzadeh@fau.de, and robert.schober@fau.de).

C. Jardin and H. Sticht are with the Institute for Biochemistry at the Friedrich-Alexander University (FAU), Erlangen, Germany (email: christophe.jardin@fau.de and heinrich.sticht@fau.de).

A. Motivation

The design of any communication system crucially depends on the characteristics of the channel under consideration. In MC systems, the impact of the channel on the number of observed molecules can be captured by the channel impulse response (CIR) which is defined as the expected number of molecules counted at the receiver at time t after the instantaneous release of a known number of molecules by the transmitter at time $t = 0$. The CIR, denoted by $\bar{c}(t)$, can be used as the basis for the design of equalization and detection schemes for MC systems [5], [6]. For diffusion-based MC, the released molecules move randomly according to Brownian motion which is caused by thermal vibration and collisions with other molecules in the fluid environment. Thereby, the average concentration of the molecules at a given coordinate $\mathbf{a} = [a_x, a_y, a_z]$ and at time t after their release by the transmitter, denoted by $\bar{C}(\mathbf{a}, t)$, is governed by Fick's second law of diffusion [5]. Finding $\bar{C}(\mathbf{a}, t)$ analytically involves solving partial differential equations and depends on initial and boundary conditions. Therefore, one possible approach for determining the CIR, which is widely employed in the literature [6], is to first derive a sufficiently accurate analytical expression for $\bar{C}(\mathbf{a}, t)$ for the considered MC channel from Fick's second law, and to subsequently integrate it over the receiver volume, V^{rec} , i.e.,

$$\bar{c}(t) = \iiint_{\mathbf{a} \in V^{\text{rec}}} \bar{C}(\mathbf{a}, t) da_x da_y da_z. \quad (1)$$

However, this approach may not be applicable in many practical scenarios as discussed in the following.

- The CIR can be obtained based on (1) only for the special case of a fully *transparent* receiver where it is assumed that the molecules move through the receiver as if it was not present in the environment. The assumption of a fully transparent receiver is a valid approximation only for some particular scenarios where the interaction of the receiver with the molecules can be neglected. However, for general receivers, the relationship between the concentration $\bar{C}(\mathbf{a}, t)$ and the number of observed molecules $\bar{c}(t)$ may not be as straightforward [7]–[9].
- Solving the differential equation associated with Fick's second law is possible only for simple and idealistic environments. For example, assuming a *point* source located at the origin of an *unbounded* environment and *impulsive* molecule release, $\bar{C}(\mathbf{a}, t)$ is obtained as [6]

$$\bar{C}(\mathbf{a}, t) = \frac{N^{\text{Tx}}}{(4\pi Dt)^{3/2}} \exp\left(-\frac{|\mathbf{a}|^2}{4Dt}\right) \left[\frac{\text{molecules}}{\text{m}^3}\right], \quad (2)$$

where N^{Tx} is the number of molecules released by the transmitter at $t = 0$ and D is the diffusion coefficient of the signaling molecule. However, $\bar{C}(\mathbf{a}, t)$ cannot be obtained in closed form for most practical MC environments which may involve difficult boundary conditions, non-instantaneous molecule release, flow, etc. Additionally, as has been shown in [10], the classical Fick's diffusion equation might even not be applicable in complex MC environments as physico-chemical interactions of the molecules with other objects in the channel, such as other molecules, cells, and microvessels, are not accounted for.

- Even if an expression for $\bar{C}(\mathbf{a}, t)$ can be obtained for a particular MC system, e.g. (2), it will be a function of several channel parameters such as the distance between the transmitter and the receiver and the diffusion coefficient. However, in practice, these parameters may not be known a priori and also have to be estimated [11], [12]. This complicates finding the CIR based on $\bar{C}(\mathbf{a}, t)$.

Fortunately, for most communication problems, including equalization and detection, only the *expected* number of molecules that the receiver observes at the sampling times is needed [5], [6]. Hence, the difficulties associated with deriving $\bar{C}(\mathbf{a}, t)$ can be avoided by directly estimating the CIR. Motivated by the above discussion, our goal in this paper is to develop a general CIR estimation framework for MC systems which is not limited to a particular MC channel model or a specific receiver type and does not require knowledge of the channel parameters.

B. Related Work

In most existing works on MC, the CIR is assumed to be perfectly known for receiver design [5], [6], [13]. In the following, we review the relevant MC literature that focused on channel characterization. Estimation of the distance between a transmitter and a receiver was studied in [11], [12], [14] for diffusive MC. In [15], an end-to-end mathematical model, including transmitter, channel, and receiver, was presented, and in [16], a stochastic channel model was proposed for flow-based and diffusion-based MC. For active transport MC, a Markov chain channel model was derived in [17]. Additionally, a unifying model including the effects of external noise sources and inter-symbol interference (ISI) was proposed for diffusive MC in [18]. In [19], the authors analyzed a microfluidic MC channel, propagation noise, and channel memory. For neuro-spike communications, a physical model for the channel between two neurons was developed in [20]. In addition to these theoretical works, experimental results for the characterization of MC channels were reported in [21], [22]. However, the focus of [11], [12], [15]–[22] is either channel modeling or the estimation of channel parameters, i.e., the obtained results are not directly applicable to CIR acquisition. In contrast to MC, for conventional wireless communication, there is a rich literature on channel estimation, mainly for linear channel models and impairment by additive white Gaussian noise (AWGN), see [23]–[25], and the references therein. Channel estimation was also studied for non-linear and/or non-AWGN channels especially in optical communication. For example, a

linear time-invariant system with chi-squared noise was used in [26] to model the optical fiber channel. However, the MC channel model considered in this paper is different from the channel models considered in [23]–[26], and hence, these results are not directly applicable to MC.

In this paper, we consider the Poisson channel which was introduced in [27], [28] for molecule-counting receivers in MC systems. The Poisson channel was previously used to model optical communication channels with photon-counting receivers, see [29] and the references therein. Moreover, the authors of a recent paper [30] adopted the Poisson channel model for non-line-of-sight (NLOS) optical wireless communication and proposed two different channel estimators. However, to the best of the authors' knowledge, channel estimation for the Poisson MC channel was first considered in the conference version of this paper [31]. We note that the channel estimators developed in this paper for MC systems are different from the channel estimators presented in [30] for NLOS optical communications. Moreover, the estimators considered in [30] do not take into account the non-negativity of the CIR coefficients. In contrast, we have carefully considered this non-negativity constraint on the CIR coefficients in the proposed estimators. Finally, in contrast to [30], we assume that the mean of the noise is unknown and has to be estimated as well. Therefore, the results in [30] are not directly applicable to the MC channel considered in this paper.

C. Contributions

In this paper, we directly estimate the CIR of the MC channel based on the channel output, i.e., the number of molecules observed at the receiver. In particular, we present a training-based CIR estimation framework which aims at estimating the CIR based on the detected number of molecules at the receiver due to the emission of a sequence of known numbers of molecules by the transmitter. Thereby, we consider the following two scenarios: *i)* Non-Bayesian CIR estimation where statistical CIR knowledge is not available or not exploited. For this case, we first derive the optimal maximum likelihood (ML) CIR estimator. Subsequently, we obtain the suboptimal least sum of square errors (LSSE) CIR estimator which entails a lower computational complexity than the ML estimator. Additionally, we derive the classical Cramer Rao (CR) bound which constitutes a lower bound on the estimation error variance of any unbiased estimator. *ii)* Bayesian CIR estimation where knowledge of the CIR statistics is available and exploited. Here, we first investigate maximum a posteriori (MAP) estimation as the optimal approach which requires full statistical knowledge of the MC channel. Subsequently, we derive the linear minimum mean square error (LMMSE) estimator for the case when only the first and second order statistics of the MC channel are available. Additionally, we derive the Bayesian CR bound as a generalization of the classical CR bound for estimators which exploit statistical channel knowledge. Finally, we study optimal and suboptimal training sequence designs for the considered MC system. Simulation results confirm the analysis and evaluate the performance of the proposed estimation techniques with respect to the corresponding CR lower bound.

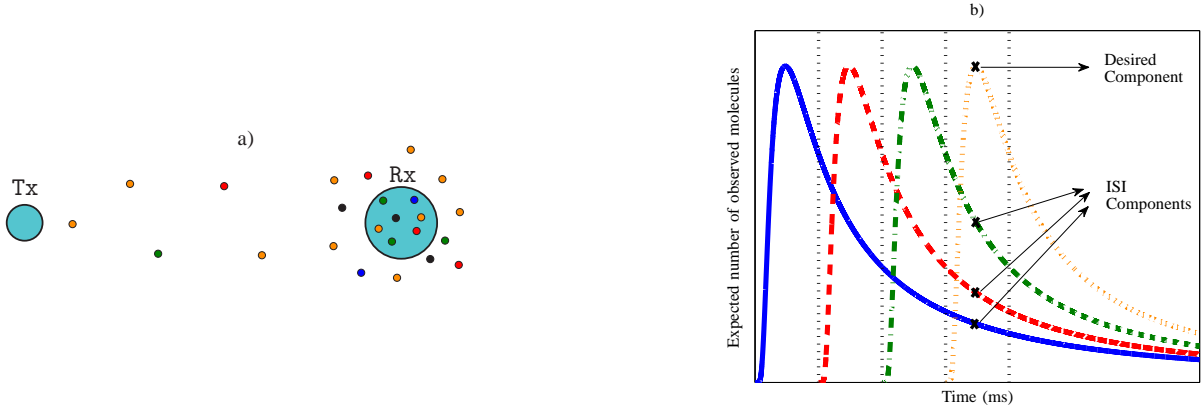


Fig. 1. a) An illustrative time snapshot of an MC system during the fourth symbol interval where the transmitted molecules in the first, second, third, and fourth symbol intervals are shown in blue, red, green, and orange colors, respectively, and noise molecules are shown in black color. b) Illustration of ISI: the expected number of observed molecules at the receiver if the transmitter emits N^{Tx} molecules at the beginning of each symbol interval. The vertical dotted lines indicate the beginning of a new symbol interval.

We note that in contrast to the conference version [31], which studies only the case when statistical channel knowledge is not exploited, this paper also provides optimal and suboptimal CIR estimators, training sequence designs, and performance bounds for the case when statistical channel knowledge is exploited. Moreover, many of the extensive discussions, simulation results, and proofs provided in this paper are not included in [31].

D. Organization and Notation

The remainder of this paper is organized as follows. In Section II, some preliminaries and assumptions are presented and the classical and Bayesian CR bounds are derived. CIR estimators which do not require statistical channel knowledge are proposed in Section III, and CIR estimators which do take advantage of statistical channel knowledge are given in Section IV. In Section V, several different training sequence designs are presented. Numerical results are provided in Section VI, and conclusions are drawn in Section VII.

Notations: We use the following notations throughout this paper: $\mathbb{E}_x\{\cdot\}$ denotes expectation with respect to random variable (RV) x , $|\cdot|$ represents the cardinality of a set, and $[x]^+ = \max\{0, x\}$. Bold capital and small letters are used to denote matrices and vectors, respectively. $\mathbf{1}$ and $\mathbf{0}$ are vectors whose elements are all ones and zeros, respectively, \mathbf{I} denotes the identity matrix, \mathbf{A}^T denotes the transpose of \mathbf{A} , $\|\mathbf{a}\|$ represents the norm of vector \mathbf{a} , $[\mathbf{A}]_{mn}$ denotes the element in the m -th row and n -th column of matrix \mathbf{A} , $\text{tr}\{\mathbf{A}\}$ is the trace of matrix \mathbf{A} , $\text{diag}\{\mathbf{a}\}$ denotes a diagonal matrix with the elements of vector \mathbf{a} on its main diagonal, $\text{vdiag}\{\mathbf{A}\}$ is a vector which contains the diagonal entries of matrix \mathbf{A} , $\text{eig}\{\mathbf{A}\}$ is the set of eigen-values of matrix \mathbf{A} , $\mathbf{A} \succeq \mathbf{0}$ denotes a positive semidefinite matrix \mathbf{A} , and $\mathbf{a} \geq \mathbf{0}$ specifies that all elements of vector \mathbf{a} are non-negative. Additionally, $\nabla_{\mathbf{a}\mathbf{a}}^2 f(\mathbf{a})$ denotes the Hessian matrix of function $f(\mathbf{a})$ with respect to vector \mathbf{a} . Furthermore, $\text{Pois}(\lambda)$ denotes a Poisson RV with mean λ , $\text{Bin}(n, p)$ denotes a binomial RV for n trials and

success probability p , and $\mathcal{N}(\mathbf{a}, \mathbf{A})$ denotes a multivariate normal RV with mean vector \mathbf{a} and covariance matrix \mathbf{A} .

II. PRELIMINARIES, ASSUMPTIONS, AND PERFORMANCE BOUNDS

In this section, we present the considered MC channel model, formulate the CIR estimation problem, and derive the corresponding classical and Bayesian CR bounds.

A. System Model

We consider an MC system consisting of a transmitter, a channel, and a receiver, see Fig. 1 a). At the beginning of each symbol interval, the transmitter releases a fraction of N^{Tx} molecules where N^{Tx} is the maximum number of molecules that the transmitter can release at once, i.e., concentration shift keying (CSK) is performed [2]. In this paper, we assume that the transmitter emits only one type of molecule. The released molecules propagate through the medium between the transmitter and the receiver. We assume that the movements of individual molecules are independent from each other. The receiver counts the number of observed molecules in each symbol interval. We note that this is a rather general model for the MC receiver which includes well-known receivers such as the transparent receiver [6], the absorbing receiver [7], and the reactive receiver [8].

Due to the memory of the MC channel, inter-symbol interference (ISI) occurs [18], [19], see Fig. 1 b). In particular, ISI-free communication is only possible if the symbol intervals are chosen sufficiently large such that the CIR fully decays to zero within one symbol interval which severely limits the transmission rate and results in an inefficient MC system design. Therefore, taking into account the effect of ISI, we assume the following input-output relation for the MC system

$$r[k] = \sum_{l=1}^L c_l[k] + c_n[k], \quad (3)$$

where $r[k]$ is the number of molecules detected at the receiver in symbol interval k , L is the number of memory taps of the channel, and $c_l[k]$ is the number of molecules observed at the receiver in symbol interval k due to the release of $s[k-l+1]N^{\text{Tx}}$ molecules by the transmitter in symbol interval $k-l+1$, where $s[k] \in [0, 1]$ is the transmitted symbol in symbol interval k . Thereby, $c_l[k]$ can be well approximated by a Poisson RV with mean $\bar{c}_l s[k-l+1]$, i.e., $c_l[k] \sim \text{Pois}(\bar{c}_l s[k-l+1])$, see [5], [27]. Moreover, $c_n[k]$ is the number of external noise molecules detected by the receiver in symbol interval k but not released by the transmitter. Noise molecules may originate from interfering sources which employ the same type of molecule as the considered MC system. Hence, $c_n[k]$ can also be modeled as a Poisson RV, i.e., $c_n[k] \sim \text{Pois}(\bar{c}_n)$, where $\bar{c}_n = \mathbb{E}\{c_n[k]\}$.

Remark 1: From a probabilistic point of view, we can assume that each molecule released by the transmitter in symbol interval $k-l+1$ is observed at the receiver in symbol interval k with a certain probability, denoted by p_l . Thereby, the probability that n molecules are observed at the receiver in symbol interval k due to the emission of N^{Tx} molecules in symbol interval $k-l+1$ follows a binomial distribution, i.e., $n \sim \text{Bin}(N^{\text{Tx}}, p_l)$. Moreover, assuming $N^{\text{Tx}} \rightarrow \infty$ while $N^{\text{Tx}} p_l \triangleq \bar{c}_l$ is fixed, the binomial distribution $\text{Bin}(N^{\text{Tx}}, p_l)$ converges to the Poisson distribution $\text{Pois}(\bar{c}_l)$ [32]. This is a valid assumption in MC since the number of released molecules is often very large to ensure that a sufficient number of molecules reaches the receiver. The same reasoning applies to the noise molecules. \square

Unlike the conventional linear input-output model for channels with memory in wireless communication systems [23], [24], the channel model in (3) is not linear since $s[k-l+1]$ does not affect the observation $r[k]$ directly but via Poisson RV $c_l[k]$. However, the *expectation* of the received signal is linearly dependent on the transmitted signal, i.e.,

$$\bar{r}[k] = \mathbb{E}\{r[k]\} = \sum_{l=1}^L \bar{c}_l s[k-l+1] + \bar{c}_n. \quad (4)$$

We note that for a given $s[k]$, in general, the actual number of molecules observed at the receiver, $r[k]$, will differ from the expected number of observed molecules, $\bar{r}[k]$, due to the intrinsic noisiness of diffusion. Here, we emphasize that the considered MC channel model is characterized by \bar{c}_l , $l = 1, \dots, L$, and \bar{c}_n , see Fig. 2, which we refer to as the CIR of the MC channel throughout the remainder of the paper.

B. CIR Estimation Problem

Let $\mathbf{s} = [s[1], s[2], \dots, s[K]]^T$ be a training sequence of length K . Here, we assume continuous transmission. Therefore, in order to ensure that the received signal is only affected by training sequence \mathbf{s} and not by the transmissions in previous symbol intervals, we only employ $r[k]$, $k \geq L$, for CIR estimation. Thereby, the $K-L+1$ samples used for CIR estimation are given by

$$r[L] = \text{Pois}(\bar{c}_1 s[L]) + \text{Pois}(\bar{c}_2 s[L-1]) + \dots$$

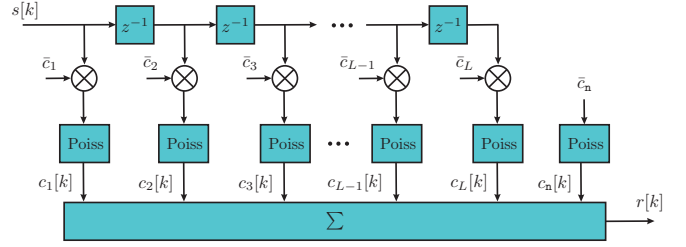


Fig. 2. Input-output signal model for an MC system with L memory taps. Here, block “ z^{-1} ” denotes one symbol interval delay and block “Pois” generates a Poisson RV with a mean equal to the input [5], [27]. The considered MC channel is characterized by \bar{c}_l , $l = 1, \dots, L$, i.e., the CIR. The goal of this paper is to estimate both the CIR and the mean of the noise, \bar{c}_n , based on RV $r[k]$.

$$+ \text{Pois}(\bar{c}_L s[1]) + \text{Pois}(\bar{c}_n) \quad (5a)$$

$$r[L+1] = \text{Pois}(\bar{c}_1 s[L+1]) + \text{Pois}(\bar{c}_2 s[L]) + \dots \\ + \text{Pois}(\bar{c}_L s[2]) + \text{Pois}(\bar{c}_n) \quad (5b)$$

$$\vdots$$

$$r[K] = \text{Pois}(\bar{c}_1 s[K]) + \text{Pois}(\bar{c}_2 s[K-1]) + \dots \\ + \text{Pois}(\bar{c}_L s[K-L+1]) + \text{Pois}(\bar{c}_n). \quad (5c)$$

For convenience of notation, we define $\mathbf{r} = [r[L], r[L+1], \dots, r[K]]^T$ and $\bar{\mathbf{c}} = [\bar{c}_1, \bar{c}_2, \dots, \bar{c}_L, \bar{c}_n]^T$, and $f_{\mathbf{r}}(\mathbf{r}|\bar{\mathbf{c}}, \mathbf{s})$ is the probability density function (PDF) of observation \mathbf{r} conditioned on a given channel $\bar{\mathbf{c}}$ and a given training sequence \mathbf{s} . We assume that the CIR¹, $\bar{\mathbf{c}}$, remains unchanged for a sufficiently large block of symbol intervals during which CIR estimation and data transmission are performed. However, the CIR may change from one block to the next due to e.g. a change of the distance between transmitter and receiver. To model this, we assume that CIR $\bar{\mathbf{c}}$ is a RV which takes its values in each block according to a PDF $f_{\bar{\mathbf{c}}}(\bar{\mathbf{c}})$. To summarize, in each block, the stochastic model in (3) is characterized by $\bar{\mathbf{c}}$ and our goal in this paper is to estimate $\bar{\mathbf{c}}$ based on the vector of random observations \mathbf{r} .

C. CR Lower Bound

The classical CR bound is a lower bound on the variance of any unbiased estimator of a *deterministic* parameter. However, this bound can be also generalized to stochastic parameters which leads to the Bayesian CR bound [32], [33]. In particular, under some regularity conditions², the covariance matrix of any unbiased estimate, $\hat{\bar{\mathbf{c}}}$, of parameter $\bar{\mathbf{c}}$, denoted by $\mathbf{C}(\hat{\bar{\mathbf{c}}})$, satisfies

$$\mathbf{C}(\hat{\bar{\mathbf{c}}}) - \mathbf{I}^{-1}(\bar{\mathbf{c}}) \succeq 0, \quad (6)$$

¹With a slight abuse of notation, we refer to vector $\bar{\mathbf{c}}$ as the CIR vector throughout the remainder of the paper although $\bar{\mathbf{c}}$ also contains the mean of the noise \bar{c}_n .

²These conditions ensure that the Fisher information matrix exists. In particular, the continuous differentiability of the PDFs $f_{\mathbf{r}}(\mathbf{r}|\bar{\mathbf{c}}, \mathbf{s})$ and $f_{\bar{\mathbf{c}}}(\bar{\mathbf{c}}|\mathbf{r}, \bar{\mathbf{c}}|\mathbf{s})$ is a sufficient condition [32].

where $\mathbf{I}(\bar{\mathbf{c}})$ is the Fisher information matrix of parameter vector $\bar{\mathbf{c}}$ and is given by [33]

$$\mathbf{I}(\bar{\mathbf{c}}) = \begin{cases} \mathbb{E}_{\mathbf{r}|\bar{\mathbf{c}}} \left\{ -\nabla_{\bar{\mathbf{c}}}^2 \ln \{ f_{\mathbf{r}}(\mathbf{r}|\bar{\mathbf{c}}, \mathbf{s}) \} \right\}, & \text{if } \bar{\mathbf{c}} \text{ is a deterministic parameter} \\ \mathbb{E}_{\mathbf{r}, \bar{\mathbf{c}}} \left\{ -\nabla_{\bar{\mathbf{c}}}^2 \ln \{ f_{\mathbf{r}, \bar{\mathbf{c}}}(\mathbf{r}, \bar{\mathbf{c}}|\mathbf{s}) \} \right\}, & \text{if } \bar{\mathbf{c}} \text{ is a stochastic parameter} \end{cases} \quad (7)$$

We assume that conditioned on $\bar{\mathbf{c}}$ and \mathbf{s} , the observations in different symbol intervals are independent, i.e., $r[k]$ is independent of $r[k']$ for $k \neq k'$. This assumption is valid in practice if the time interval between two consecutive samples is sufficiently large, see [5] for a detailed discussion. Moreover, from (3), we observe that $r[k]$ is a sum of Poisson RVs. Hence, $r[k]$ is also a Poisson RV with its mean equal to the sum of the means of the summands, i.e., $r[k] \sim \text{Poiss}(\bar{r}[k])$ with $\bar{r}[k] = \bar{c}_n + \sum_{l=1}^L \bar{c}_l s[k-l+1] = \bar{\mathbf{c}}^T \mathbf{s}_k$ and $\mathbf{s}_k = [s[k], s[k-1], \dots, s[k-L+1], 1]^T$. Therefore, $f_{\mathbf{r}}(\mathbf{r}|\bar{\mathbf{c}}, \mathbf{s})$ is given by

$$f_{\mathbf{r}}(\mathbf{r}|\bar{\mathbf{c}}, \mathbf{s}) = \prod_{k=L}^K \frac{(\bar{\mathbf{c}}^T \mathbf{s}_k)^{r[k]} \exp(-\bar{\mathbf{c}}^T \mathbf{s}_k)}{r[k]!}. \quad (8)$$

For a positive semidefinite matrix, the diagonal elements are non-negative, i.e., $[\mathbf{C}(\hat{\bar{\mathbf{c}}}) - \mathbf{I}^{-1}(\bar{\mathbf{c}})]_{i,i} \geq 0$. Therefore, for an unbiased estimator, i.e., $\mathbb{E}\{\hat{\bar{\mathbf{c}}}\} = \bar{\mathbf{c}}$ holds, with the estimation error vector defined as $\mathbf{e} = \bar{\mathbf{c}} - \hat{\bar{\mathbf{c}}}$, the classical CR bound for deterministic $\bar{\mathbf{c}}$ provides the following lower bound on the sum of the expected square errors

$$\begin{aligned} & \mathbb{E}_{\mathbf{r}|\bar{\mathbf{c}}} \{ \|\mathbf{e}\|^2 \} \\ & \geq \text{tr} \{ \mathbf{I}^{-1}(\bar{\mathbf{c}}) \} = \text{tr} \left\{ \left[\sum_{k=L}^K \frac{\mathbf{s}_k \mathbf{s}_k^T}{\bar{\mathbf{c}}^T \mathbf{s}_k} \right]^{-1} \right\} \triangleq \text{CCRB}(\bar{\mathbf{c}}), \end{aligned} \quad (9)$$

where $\text{CCRB}(\bar{\mathbf{c}})$ denotes the classical CR bound for a given fixed/deterministic parameter $\bar{\mathbf{c}}$.

On the other hand, the Bayesian CR bound for stochastic $\bar{\mathbf{c}}$ is given by

$$\begin{aligned} & \mathbb{E}_{\mathbf{r}, \bar{\mathbf{c}}} \{ \|\mathbf{e}\|^2 \} \\ & \geq \text{tr} \left\{ \left[\mathbb{E}_{\bar{\mathbf{c}}} \left\{ -\nabla_{\bar{\mathbf{c}}}^2 \ln \{ f_{\bar{\mathbf{c}}}(\bar{\mathbf{c}}) \} + \sum_{k=L}^K \frac{\mathbf{s}_k \mathbf{s}_k^T}{\bar{\mathbf{c}}^T \mathbf{s}_k} \right\} \right]^{-1} \right\} \triangleq \text{BCRB}. \end{aligned} \quad (10)$$

The expectation in (10) is taken over RV $\bar{\mathbf{c}}$ which takes its values according to PDF $f_{\bar{\mathbf{c}}}(\bar{\mathbf{c}})$. Note that $f_{\bar{\mathbf{c}}}(\bar{\mathbf{c}})$ depends on the MC environment and a general analytical expression for $f_{\bar{\mathbf{c}}}(\bar{\mathbf{c}})$ is not yet available in the literature. In practice, $f_{\bar{\mathbf{c}}}(\bar{\mathbf{c}})$ can be obtained using historical measurements of the CIR, see Remark 8 for further discussion.

Remark 2: By comparing (9) and (10), we observe that $\mathbb{E}_{\bar{\mathbf{c}}} \{ \text{CCRB}(\bar{\mathbf{c}}) \} \geq \text{BCRB}$ holds as a result of Jensen's inequality [34]. In particular, for unbiased estimators which do not exploit any statistical knowledge of the MC channel, both lower bounds $\mathbb{E}_{\bar{\mathbf{c}}} \{ \text{CCRB}(\bar{\mathbf{c}}) \}$ and BCRB are valid but $\mathbb{E}_{\bar{\mathbf{c}}} \{ \text{CCRB}(\bar{\mathbf{c}}) \}$ is a tighter bound. On the other hand, for unbiased estimators which exploit some statistical knowledge of the MC channel, $\mathbb{E}_{\bar{\mathbf{c}}} \{ \text{CCRB}(\bar{\mathbf{c}}) \}$ is not a valid lower bound whereas BCRB is a valid lower bound. \square

III. CIR ESTIMATION WITHOUT STATISTICAL CHANNEL KNOWLEDGE

In this section, we consider estimators which do not exploit statistical knowledge of the MC channel. In particular, we derive the ML and the LSSE CIR estimators.

A. ML CIR Estimation

The ML CIR estimator finds the CIR estimate which maximizes the likelihood of observation vector \mathbf{r} [32]. In particular, the ML estimator is given by

$$\hat{\bar{\mathbf{c}}}^{\text{ML}} = \underset{\bar{\mathbf{c}} \geq \mathbf{0}}{\text{argmax}} f_{\mathbf{r}}(\mathbf{r}|\bar{\mathbf{c}}, \mathbf{s}), \quad (11)$$

where $f_{\mathbf{r}}(\mathbf{r}|\bar{\mathbf{c}}, \mathbf{s})$ is given in (8). Maximizing $f_{\mathbf{r}}(\mathbf{r}|\bar{\mathbf{c}}, \mathbf{s})$ is equivalent to maximizing $\ln(f_{\mathbf{r}}(\mathbf{r}|\bar{\mathbf{c}}, \mathbf{s}))$ since $\ln(\cdot)$ is a monotonically increasing function. Hence, the ML estimate can be rewritten as

$$\begin{aligned} \hat{\bar{\mathbf{c}}}^{\text{ML}} &= \underset{\bar{\mathbf{c}} \geq \mathbf{0}}{\text{argmax}} g(\bar{\mathbf{c}}) \quad \text{where} \\ g(\bar{\mathbf{c}}) &\triangleq \sum_{k=L}^K \left[-\bar{\mathbf{c}}^T \mathbf{s}_k + r[k] \ln(\bar{\mathbf{c}}^T \mathbf{s}_k) \right]. \end{aligned} \quad (12)$$

To present the solution of the above optimization problem rigorously, we first define some auxiliary variables. Let $\mathcal{A} = \{\mathcal{A}_1, \mathcal{A}_2, \dots, \mathcal{A}_N\}$ denote a set which contains all possible $N = 2^{L+1} - 1$ subsets of set $\mathcal{F} = \{1, 2, \dots, L, n\}$ except for the empty set. Here, \mathcal{A}_n , $n = 1, 2, \dots, N$, denotes the n -th subset of \mathcal{A} . Moreover, let $\bar{\mathbf{c}}^{\mathcal{A}_n}$ and $\mathbf{s}_k^{\mathcal{A}_n}$ denote reduced-dimension versions of $\bar{\mathbf{c}}$ and \mathbf{s}_k , respectively, which contain only those elements of $\bar{\mathbf{c}}$ and \mathbf{s}_k whose indices are elements of set \mathcal{A}_n , respectively.

Lemma 1: The ML estimator of the CIR for the considered MC channel is given by Algorithm 1 where the following nonlinear system of equations is solved³ for different \mathcal{A}_n

$$\sum_{k=L}^K \left[\frac{r[k]}{(\bar{\mathbf{c}}^{\mathcal{A}_n})^T \mathbf{s}_k^{\mathcal{A}_n}} - 1 \right] \mathbf{s}_k^{\mathcal{A}_n} = \mathbf{0}. \quad (13)$$

Proof: Please refer to Appendix A. \blacksquare

Remark 3: Recall that in the system model, we assumed a priori L non-zero taps and a noise with non-zero mean, i.e., $\bar{\mathbf{c}} > \mathbf{0}$. Moreover, the consistency property of ML estimation [32, Chapter 4] implies that under some regularity conditions, notably that the likelihood is a continuous function of $\bar{\mathbf{c}}$ and that $\bar{\mathbf{c}}$ is not on the boundary of the parameter set $\bar{\mathbf{c}} \geq \mathbf{0}$, we obtain $\hat{\bar{\mathbf{c}}}^{\text{ML}} \rightarrow \bar{\mathbf{c}}$ as $K \rightarrow \infty$. As a result, the ML estimator is asymptotically unbiased. Therefore, for large values of K , the ML estimator becomes sufficiently accurate such that none of the elements of $\hat{\bar{\mathbf{c}}}^{\text{ML}}$ is zero. In this case, Algorithm 1 reduces to directly solving (13) for $\mathcal{A}_n = \mathcal{F}$, where the left-hand side of (13) is the derivative of $g(\bar{\mathbf{c}})$ given in (12) with respect to $\bar{\mathbf{c}}$. \square

Motivated by the results in Lemma 1 and the discussion in Remark 3, we propose the following simpler but suboptimal estimate based on the ML estimate in (13).

³A system of nonlinear equations can be solved using mathematical software packages, e.g. Mathematica.

Algorithm 1 ML/LSSE CIR Estimate $\hat{\mathbf{c}}^{\text{ML}}/\hat{\mathbf{c}}^{\text{LSSE}}$

initialize $\mathcal{A}_n = \mathcal{F}$ and solve (13)/(17) to find $\bar{\mathbf{c}}^{\mathcal{F}}$
if $\bar{\mathbf{c}}^{\mathcal{F}} \geq \mathbf{0}$ **then**
 Set $\hat{\mathbf{c}}^{\text{ML}} = \bar{\mathbf{c}}^{\mathcal{F}}/\hat{\mathbf{c}}^{\text{LSSE}} = \bar{\mathbf{c}}^{\mathcal{F}}$
else
 for $\forall \mathcal{A}_n \neq \mathcal{F}$ **do**
 Solve (13)/(17) to find $\bar{\mathbf{c}}^{\mathcal{A}_n}$
 if $\bar{\mathbf{c}}^{\mathcal{A}_n} \geq \mathbf{0}$ **holds then**
 Set the values of the elements of $\hat{\mathbf{c}}^{\text{CAN}}$, whose indices
 are in \mathcal{A}_n , equal to the values of the corresponding
 elements in $\bar{\mathbf{c}}^{\mathcal{A}_n}$ and the remaining $L + 1 - |\mathcal{A}_n|$
 elements equal to zero;
 Save $\hat{\mathbf{c}}^{\text{CAN}}$ in the candidate set \mathcal{C}
 else
 Discard $\bar{\mathbf{c}}^{\mathcal{A}_n}$
 end if
 end for
 Choose $\hat{\mathbf{c}}^{\text{ML}}/\hat{\mathbf{c}}^{\text{LSSE}}$ equal to that $\hat{\mathbf{c}}^{\text{CAN}}$ in the candidate set
 \mathcal{C} which **maximizes** $g(\bar{\mathbf{c}})$ /**minimizes** $\|\boldsymbol{\epsilon}\|^2$
end if

Suboptimal ML-Based CIR Estimation: For a given observation vector \mathbf{r} , the suboptimal estimate $\hat{\mathbf{c}}_{\text{sub}}^{\text{ML}}$ is given by $\hat{\mathbf{c}}_{\text{sub}}^{\text{ML}} = [\bar{\mathbf{c}}]^+$ where $\bar{\mathbf{c}}$ is the solution of the following system of equations

$$\sum_{k=L}^K \left[\frac{r[k]}{\bar{\mathbf{c}}^T \mathbf{s}_k} - 1 \right] \mathbf{s}_k = \mathbf{0}. \quad (14)$$

Note that the above estimate is simpler than the optimal ML estimate in Lemma 1 since in the case that the $\bar{\mathbf{c}}$ found from (14) does not satisfy $\bar{\mathbf{c}} \geq \mathbf{0}$, we do not search for the optimal boundary points and instead just set the negative elements of $\bar{\mathbf{c}}$ to zero. Moreover, considering Remark 3, this simpler estimate becomes asymptotically identical to the ML estimate, i.e., as $K \rightarrow \infty$, we obtain $\hat{\mathbf{c}}_{\text{sub}}^{\text{ML}} \rightarrow \hat{\mathbf{c}}^{\text{ML}}$. As we will see in Section VI, cf. Fig. 4, $\hat{\mathbf{c}}_{\text{sub}}^{\text{ML}}$ approaches the performance of $\hat{\mathbf{c}}^{\text{ML}}$ even for small K .

Remark 4: We note that obtaining the ML estimate of the CIR might be computationally challenging for practical MC systems as nanonodes have limited computational power. Nevertheless, ML estimation can serve as a benchmark for low-complexity estimators such as the LSSE estimator. Moreover, for applications where the nanoreceiver only collects observations, i.e., vector \mathbf{r} , and forwards them to an external processing unit outside the MC environment, the computational complexity of ML estimation may be affordable. This case may apply e.g. in health monitoring when a computer outside the body may be available for offline processing. \square

B. LSSE CIR Estimation

The LSSE CIR estimator chooses that $\bar{\mathbf{c}}$ which minimizes the sum of the square errors for observation vector \mathbf{r} . Thereby, the error vector is defined as $\boldsymbol{\epsilon} = \mathbf{r} - \mathbb{E}\{\mathbf{r}\} = \mathbf{r} - \mathbf{S}\bar{\mathbf{c}}$ where $\mathbf{S} = [\mathbf{s}_L, \mathbf{s}_{L+1}, \dots, \mathbf{s}_K]^T$. In particular, the LSSE CIR estimate can

be formally written as

$$\hat{\mathbf{c}}^{\text{LSSE}} = \underset{\bar{\mathbf{c}} \geq \mathbf{0}}{\operatorname{argmin}} \|\boldsymbol{\epsilon}\|^2. \quad (15)$$

Here, the square norm of the error vector is obtained as

$$\begin{aligned} \|\boldsymbol{\epsilon}\|^2 &= \operatorname{tr}\{\boldsymbol{\epsilon}\boldsymbol{\epsilon}^T\} = \operatorname{tr}\{(\mathbf{r} - \mathbf{S}\bar{\mathbf{c}})(\mathbf{r} - \mathbf{S}\bar{\mathbf{c}})^T\} \\ &= \operatorname{tr}\{\mathbf{S}^T \mathbf{S} \bar{\mathbf{c}} \bar{\mathbf{c}}^T\} - 2\operatorname{tr}\{\mathbf{r}^T \mathbf{S} \bar{\mathbf{c}}\} + \operatorname{tr}\{\mathbf{r} \mathbf{r}^T\}, \end{aligned} \quad (16)$$

where we used the following properties of the trace: $\operatorname{tr}\{\mathbf{A}\} = \operatorname{tr}\{\mathbf{A}^T\}$ and $\operatorname{tr}\{\mathbf{A}\mathbf{B}\} = \operatorname{tr}\{\mathbf{B}\mathbf{A}\}$ [35]. The LSSE estimate is given in the following lemma where we use the auxiliary matrix $\mathbf{S}^{\mathcal{A}_n} = [\mathbf{s}_L^{\mathcal{A}_n}, \mathbf{s}_{L+1}^{\mathcal{A}_n}, \dots, \mathbf{s}_K^{\mathcal{A}_n}]^T$.

Lemma 2: The LSSE estimator of the CIR for the considered MC channel is given by Algorithm 1 where for a given set \mathcal{A}_n , $\bar{\mathbf{c}}^{\mathcal{A}_n}$ is obtained as

$$\bar{\mathbf{c}}^{\mathcal{A}_n} = ((\mathbf{S}^{\mathcal{A}_n})^T \mathbf{S}^{\mathcal{A}_n})^{-1} (\mathbf{S}^{\mathcal{A}_n})^T \mathbf{r}. \quad (17)$$

Proof: Please refer to Appendix B. \blacksquare

Remark 5: The LSSE estimator employs in fact a linear matrix multiplication to compute $\bar{\mathbf{c}}^{\mathcal{A}_n}$, i.e., $\bar{\mathbf{c}}^{\mathcal{A}_n} = \mathbf{F}^{\mathcal{A}_n} \mathbf{r}$ where $\mathbf{F}^{\mathcal{A}_n} = ((\mathbf{S}^{\mathcal{A}_n})^T \mathbf{S}^{\mathcal{A}_n})^{-1} (\mathbf{S}^{\mathcal{A}_n})^T$. Moreover, since the training sequence \mathbf{s} is fixed, matrix $\mathbf{F}^{\mathcal{A}_n}$ can be calculated offline and then be used for online CIR estimation. Therefore, the calculation of $\bar{\mathbf{c}}^{\mathcal{A}_n}$ for the LSSE estimator in (17) is considerably less computationally complex than the computation of $\bar{\mathbf{c}}^{\mathcal{A}_n}$ for the ML estimator in (13) which requires solving a system of nonlinear equations. \square

Corollary 1: The LSSE estimator in Lemma 2 is biased in general but asymptotically, as $K \rightarrow \infty$, becomes unbiased. More precisely, the LSSE estimator in Lemma 2 is a consistent estimator, i.e., $\hat{\mathbf{c}}^{\text{LSSE}} \rightarrow \bar{\mathbf{c}}$ as $K \rightarrow \infty$.

Proof: Please refer to Appendix C. \blacksquare

The above corollary reveals that similar to the ML estimate, the LSSE estimate is biased for short length sequences but becomes asymptotically unbiased as the sequence length grows to infinity. Moreover, motivated by the results in Corollary 1 and similar to the sub-optimal estimator proposed based on the ML estimate, we propose the following suboptimal estimator based on the LSSE estimate in (17).

Suboptimal LSSE-Based CIR Estimation: For a given observation vector \mathbf{r} , the suboptimal estimate $\hat{\mathbf{c}}_{\text{sub}}^{\text{LSSE}}$ is given by

$$\hat{\mathbf{c}}_{\text{sub}}^{\text{LSSE}} = \left[(\mathbf{S}^T \mathbf{S})^{-1} \mathbf{S}^T \mathbf{r} \right]^+. \quad (18)$$

Note that the above suboptimal estimate asymptotically, as $K \rightarrow \infty$, converges to the LSSE estimate, i.e., $\hat{\mathbf{c}}_{\text{sub}}^{\text{LSSE}} \rightarrow \hat{\mathbf{c}}^{\text{LSSE}}$. Moreover, as we will see in Section VI, cf. Fig. 4, $\hat{\mathbf{c}}_{\text{sub}}^{\text{LSSE}}$ approaches the performance of $\hat{\mathbf{c}}^{\text{LSSE}}$ even for small K .

Remark 6: We note that for finite K , the ML and LSSE estimators in Algorithm 1 are biased in general. The proposed estimators are biased because of the non-negativity of the unknown parameters. Exploiting this information in the proposed estimators causes the biasedness for small K but improves the estimation performance by reducing the variance of the estimation error. Hence, the error variances of the ML and LSSE estimates may fall below the classical CR bound. However, as $K \rightarrow \infty$, the ML and LSSE estimators become asymptotically unbiased, cf. Remark 3 and Corollary 1, and

the classical CR bound becomes a valid lower bound. The asymptotic unbiasedness of the proposed estimators is also numerically verified in Section VI, cf. Fig. 3. \square

Remark 7: The appropriate length of the training sequence depends on the required CIR accuracy and the coherence time of the MC channel. In particular, shorter training sequences can be used if higher estimation errors can be tolerated. Furthermore, since the coherence time of the MC channel determines how fast the MC channel changes, the length of the training sequence should be chosen small compared to the coherence time such that the CIR acquisition overhead is low. \square

IV. CIR ESTIMATION WITH STATISTICAL CHANNEL KNOWLEDGE

In this section, we first present the MAP estimator assuming that full statistical knowledge of the MC channel is available. Subsequently, we derive the LMMSE estimator for the case when only the first and second order statistics of the MC channel are available.

A. MAP CIR Estimation

The MAP CIR estimator is the optimal estimator assuming that full statistical knowledge of the MC channel is available, i.e., $f_{\bar{\mathbf{c}}}(\bar{\mathbf{c}})$. In particular, the MAP CIR estimator chooses that CIR $\bar{\mathbf{c}}$ which maximizes the posterior expected value of observation vector \mathbf{r} , i.e., $f_{\bar{\mathbf{c}}}(\bar{\mathbf{c}}|\mathbf{r}, \mathbf{s})$. Thereby, the MAP estimate is given by

$$\hat{\bar{\mathbf{c}}}^{\text{MAP}} = \underset{\bar{\mathbf{c}} \geq \mathbf{0}}{\text{argmax}} f_{\bar{\mathbf{c}}}(\bar{\mathbf{c}}|\mathbf{r}, \mathbf{s}) \stackrel{(a)}{=} \frac{f_{\mathbf{r}}(\mathbf{r}|\bar{\mathbf{c}}, \mathbf{s})f_{\bar{\mathbf{c}}}(\bar{\mathbf{c}})}{f_{\mathbf{r}}(\mathbf{r})}, \quad (19)$$

where (a) follows the Bayes' Theorem [32]. Note that the term $f_{\mathbf{r}}(\mathbf{r})$ does not depend on the estimate $\bar{\mathbf{c}}$. Moreover, considering that $\ln(\cdot)$ is a monotonically increasing function, the MAP estimate can be rewritten in the following convenient form

$$\hat{\bar{\mathbf{c}}}^{\text{MAP}} = \underset{\bar{\mathbf{c}} \geq \mathbf{0}}{\text{argmax}} [g(\bar{\mathbf{c}}) + \ln(f_{\bar{\mathbf{c}}}(\bar{\mathbf{c}}))], \quad (20)$$

where $g(\bar{\mathbf{c}})$ is given in (12).

Remark 8: The PDF $f_{\bar{\mathbf{c}}}(\bar{\mathbf{c}})$ depends on the considered MC environment and a general analytical expression for $f_{\bar{\mathbf{c}}}(\bar{\mathbf{c}})$ is not yet available in the literature. In practice, $f_{\bar{\mathbf{c}}}(\bar{\mathbf{c}})$ for a particular MC channel can be obtained using historical measurements of $\bar{\mathbf{c}}$. Another convenient approximation for mathematical derivations is to assume a particular shape for $f_{\bar{\mathbf{c}}}(\bar{\mathbf{c}})$ and adjust the parameters of the PDF to match the experimental data. For the simulation results presented in Section VI, we assume that $f_{\bar{\mathbf{c}}}(\bar{\mathbf{c}})$ is a multivariate Gaussian PDF⁴ with a certain mean vector $\boldsymbol{\mu}_{\bar{\mathbf{c}}}$ and covariance matrix $\Phi_{\bar{\mathbf{c}}\bar{\mathbf{c}}}$ which are chosen based on our simulation parameters. However, we emphasize that the choice of the CIR distribution

⁴We note that $\bar{\mathbf{c}} \geq \mathbf{0}$ has to hold, whereas a Gaussian PDF may lead to negative-valued realizations for the elements of $\bar{\mathbf{c}}$. To resolve this issue, in Section VI, we use $\bar{\mathbf{c}} = [\bar{\mathbf{c}}^{\text{Gaus}}]^+$, where $\bar{\mathbf{c}}^{\text{Gaus}}$ is a Gaussian distributed vector. Thereby, for mathematical tractability of computing $\hat{\bar{\mathbf{c}}}^{\text{MAP}}$, we adopt the Gaussian PDF $f_{\bar{\mathbf{c}}^{\text{Gaus}}}(\bar{\mathbf{c}}^{\text{Gaus}})$ as an approximation for $f_{\bar{\mathbf{c}}}(\bar{\mathbf{c}})$.

depends on the specific MC channel. Here, as an example, we adopt the Gaussian distribution for the PDF of the CIR. \square

Similar to the ML and LSSE estimates provided in the previous section, the optimal MAP estimate is either a stationary point or a boundary point, see Algorithm 1. Here, we do not provide a detailed solution for the MAP estimate due to space constraints, instead, we highlight the main steps for the case when the solution is a stationary point. For the case when the solution is a boundary point, we can employ the same methodology as in Algorithm 1 to find $\hat{\bar{\mathbf{c}}}^{\text{MAP}}$. In particular, the stationary points of the cost function in (20) are obtained by equating its derivative to zero, i.e., $\frac{\partial g(\bar{\mathbf{c}})}{\partial \bar{\mathbf{c}}} + \frac{\partial \ln(f_{\bar{\mathbf{c}}}(\bar{\mathbf{c}}))}{\partial \bar{\mathbf{c}}} = \mathbf{0}$. Note that the first term $\frac{\partial g(\bar{\mathbf{c}})}{\partial \bar{\mathbf{c}}}$ is given on the left-hand side of (13) for $\mathcal{A}_n = \mathcal{F}$ and the second term is given by $\frac{\partial \ln(f_{\bar{\mathbf{c}}}(\bar{\mathbf{c}}))}{\partial \bar{\mathbf{c}}} = -\frac{1}{2} (\Phi_{\bar{\mathbf{c}}\bar{\mathbf{c}}}^{-1} + \Phi_{\bar{\mathbf{c}}\bar{\mathbf{c}}}^{-T}) (\bar{\mathbf{c}} - \boldsymbol{\mu}_{\bar{\mathbf{c}}})$ for the considered Gaussian PDF $f_{\bar{\mathbf{c}}}(\bar{\mathbf{c}})$. We note that although the complexity of the MAP estimator may not be affordable for practical MC systems, we can still use it as a benchmark scheme to evaluate the performance of less complex estimators, e.g., the LMMSE estimator.

B. LMMSE CIR Estimation

The MAP estimator in (20) requires full knowledge of the channel statistics, i.e., $f_{\bar{\mathbf{c}}}(\bar{\mathbf{c}})$, which is difficult to obtain for practical MC channels, cf Remark 8. Therefore, in the following, we consider an LMMSE-based estimator which requires only knowledge of the first and second order statistics of the MC channel. In particular, in estimation theory, the average square norm of the estimation error $\mathbf{e} = \bar{\mathbf{c}} - \hat{\bar{\mathbf{c}}}$ is often adopted as performance metric, i.e., $\mathbb{E} \{ \|\mathbf{e}\|^2 \}$. Therefore, one can design an LMMSE estimator which directly minimizes $\mathbb{E} \{ \|\mathbf{e}\|^2 \}$. We note that the estimation error has to be averaged over both \mathbf{r} and $\bar{\mathbf{c}}$, i.e., $\mathbb{E}_{\mathbf{r}, \bar{\mathbf{c}}} \{ \|\mathbf{e}\|^2 \}$, since both are randomly changing, and hence, have to be modeled as RVs. In this paper, we consider an LMMSE-based estimator given by $\hat{\bar{\mathbf{c}}}^{\text{LMMSE}} = [\mathbf{F}^{\text{MMSE}} \mathbf{r}]^+$ where \mathbf{F}^{MMSE} is the MMSE matrix. Moreover, for mathematical tractability, we optimize \mathbf{F}^{MMSE} such that an upper bound on the estimation error is minimized, i.e.,

$$\mathbf{F}^{\text{MMSE}} = \underset{\mathbf{F}}{\text{argmin}} \mathbb{E}_{\mathbf{r}, \bar{\mathbf{c}}} \{ \|\mathbf{e}_{\text{up}}^{\text{MMSE}}\|^2 \}, \quad (21)$$

where $\mathbf{e}_{\text{up}}^{\text{MMSE}} = \bar{\mathbf{c}} - \hat{\bar{\mathbf{c}}}_{\text{up}}^{\text{MMSE}}$ and $\hat{\bar{\mathbf{c}}}_{\text{up}}^{\text{MMSE}} = \mathbf{F}^{\text{MMSE}} \mathbf{r}$. Note that $\hat{\bar{\mathbf{c}}}_{\text{up}}^{\text{MMSE}}$ yields an upper bound on the estimation error of $\hat{\bar{\mathbf{c}}}^{\text{MMSE}}$ because we neglect the side information that the CIR coefficients have to be non-negative by dropping $[\cdot]^+$. Hereby, $\mathbb{E}_{\mathbf{r}, \bar{\mathbf{c}}} \{ \|\mathbf{e}_{\text{up}}^{\text{MMSE}}\|^2 \}$ is obtained as

$$\begin{aligned} \mathbb{E}_{\mathbf{r}, \bar{\mathbf{c}}} \{ \|\mathbf{e}_{\text{up}}^{\text{MMSE}}\|^2 \} &= \mathbb{E}_{\mathbf{r}, \bar{\mathbf{c}}} \left\{ \text{tr} \left\{ \mathbf{e}_{\text{up}}^{\text{MMSE}} (\mathbf{e}_{\text{up}}^{\text{MMSE}})^T \right\} \right\} \\ &= \mathbb{E}_{\mathbf{r}, \bar{\mathbf{c}}} \left\{ \text{tr} \left\{ (\mathbf{F}\mathbf{r} - \bar{\mathbf{c}})(\mathbf{F}\mathbf{r} - \bar{\mathbf{c}})^T \right\} \right\} \\ &= \text{tr} \left\{ \mathbf{F} \Phi_{\mathbf{r}\mathbf{r}} \mathbf{F}^T - \mathbf{F} \Phi_{\mathbf{r}\bar{\mathbf{c}}} - \Phi_{\bar{\mathbf{c}}\mathbf{r}} \mathbf{F}^T + \Phi_{\bar{\mathbf{c}}\bar{\mathbf{c}}} \right\}, \quad (22) \end{aligned}$$

where

$$\begin{aligned} \Phi_{\mathbf{r}\mathbf{r}} &= \mathbb{E}_{\bar{\mathbf{c}}} \mathbb{E}_{\mathbf{r}|\bar{\mathbf{c}}} \{ \mathbf{r}\mathbf{r}^T \} = \mathbb{E}_{\bar{\mathbf{c}}} \{ \mathbf{S}\bar{\mathbf{c}}\bar{\mathbf{c}}^T \mathbf{S}^T + \text{diag} \{ \mathbf{S}\bar{\mathbf{c}} \} \} \\ &= \mathbf{S} \Phi_{\bar{\mathbf{c}}\bar{\mathbf{c}}} \mathbf{S}^T + \text{diag} \{ \mathbf{S} \boldsymbol{\mu}_{\bar{\mathbf{c}}} \} \end{aligned} \quad (23a)$$

$$\Phi_{\bar{\mathbf{c}}\mathbf{r}} = \Phi_{\mathbf{r}\bar{\mathbf{c}}}^T = \mathbb{E}_{\bar{\mathbf{c}}} \mathbb{E}_{\mathbf{r}|\bar{\mathbf{c}}} \{ \mathbf{r}\bar{\mathbf{c}}^T \} = \mathbb{E}_{\bar{\mathbf{c}}} \{ \mathbf{S}\bar{\mathbf{c}}\bar{\mathbf{c}}^T \} = \mathbf{S} \Phi_{\bar{\mathbf{c}}\bar{\mathbf{c}}}, \quad (23b)$$

and $\boldsymbol{\mu}_{\bar{\mathbf{c}}} = \mathbb{E}_{\bar{\mathbf{c}}}\{\bar{\mathbf{c}}\}$ and $\boldsymbol{\Phi}_{\bar{\mathbf{c}}\bar{\mathbf{c}}} = \mathbb{E}_{\bar{\mathbf{c}}}\{\bar{\mathbf{c}}\bar{\mathbf{c}}^T\}$. In addition, in (23a) and (23b), we use $\mathbb{E}_{\mathbf{X}}\{\text{tr}\{\mathbf{A}\mathbf{X}\mathbf{B}\}\} = \text{tr}\{\mathbf{A}\mathbb{E}_{\mathbf{X}}\{\mathbf{X}\}\mathbf{B}\}$, which holds for general matrices \mathbf{A} , \mathbf{B} , and \mathbf{X} . Furthermore, in (23a), we use $\mathbb{E}_{\mathbf{x}}\{\mathbf{x}\mathbf{x}^T\} = \boldsymbol{\lambda}\boldsymbol{\lambda}^T + \text{diag}\{\boldsymbol{\lambda}\}$, which is valid for multivariate Poisson random vectors \mathbf{x} with covariance matrix $\mathbf{C}(\mathbf{x}) = \text{diag}\{\boldsymbol{\lambda}\}$. The optimal MMSE matrix is given in the following lemma.

Lemma 3: For the LMMSE-based estimator $\hat{\mathbf{c}}^{\text{MMSE}} = [\mathbf{F}^{\text{MMSE}}\mathbf{r}]^+$, the optimal matrix \mathbf{F}^{MMSE} , i.e., the solution of the optimization problem in (21), is given by

$$\mathbf{F}^{\text{MMSE}} = \boldsymbol{\Phi}_{\bar{\mathbf{c}}\bar{\mathbf{c}}}^T \mathbf{S}^T (\mathbf{S}\boldsymbol{\Phi}_{\bar{\mathbf{c}}\bar{\mathbf{c}}}\mathbf{S}^T + \text{diag}\{\mathbf{S}\boldsymbol{\mu}_{\bar{\mathbf{c}}}\})^{-1}. \quad (24)$$

Proof: Please refer to Appendix D. \blacksquare

Remark 9: Note that the optimal MMSE matrix depends only on the training sequence and the first and second order channel statistics. Thus, the MMSE matrix can be computed offline once and then be used for online CIR acquisition as long as the channel statistics remain constant. Since the statistics of the CIR, $\bar{\mathbf{c}}$, change much less frequently than the CIR itself, an infrequent update of the MMSE matrix is sufficient. As we will see in Section VI, the LMMSE estimator provides a considerable performance gain compared to the ML and LSSE estimators at the cost of acquiring the required knowledge of the MC channel statistics. \square

Remark 10: Similar to the discussion regarding the ML and LSSE estimators in Remark 6, we note that the proposed MAP and LMMSE estimators are in general biased for short sequence lengths and become asymptotically unbiased as $K \rightarrow \infty$. Therefore, the Bayesian CR bound in (10) may not be a valid lower bound for the MAP and LMMSE estimators for small values of K , however, for $K \rightarrow \infty$, it becomes asymptotically a valid lower bound. Due to space constraints, we skip the detailed proofs for the biasedness and asymptotic unbiasedness of the proposed MAP and LMMSE estimators. Instead, we numerically illustrate these properties in Section VI, cf. Fig. 3. \square

V. TRAINING SEQUENCE DESIGN

In this section, we first present two optimal training sequence designs for CIR estimation in MC systems based on the LSSE and LMMSE estimators. Subsequently, we propose a suboptimal and simple training sequence which is suitable for practical applications where the involved nanomachines have limited computational processing capability. For future reference, let \mathcal{S} and \mathcal{S}^K denote the sets of all CSK symbols and all possible training sequences, respectively.

A. LSSE-Based Training Sequence Design

We first consider a training sequence design which minimizes an *upper bound* on the *average* estimation error of the LSSE estimator. First, we note that for training sequence design, the estimation error has to be averaged over both \mathbf{r} and $\bar{\mathbf{c}}$ since both are a priori unknown, and hence, have to be modeled as RVs. Again, we recall that in the system model, we assumed a priori L non-zero taps and a noise with non-zero mean. Therefore, neglecting the information that $\bar{\mathbf{c}} \geq \mathbf{0}$ has to hold in (15) yields an upper bound on the estimation

error for the LSSE estimator. This upper bound is adopted here for the problem of sequence design since the solution of (15) after dropping constraint $\bar{\mathbf{c}} \geq \mathbf{0}$ leads to the simple and elegant closed-form solution $\hat{\mathbf{c}}_{\text{up}}^{\text{LSSE}} = (\mathbf{S}^T \mathbf{S})^{-1} \mathbf{S} \mathbf{r}$, which we can employ to find optimal training sequences. Moreover, this upper bound is tight as $K \rightarrow \infty$ since $\hat{\mathbf{c}}^{\text{LSSE}} > \mathbf{0}$ holds and we obtain $\hat{\mathbf{c}}^{\text{LSSE}} = \hat{\mathbf{c}}_{\text{up}}^{\text{LSSE}}$. In Section VI, Fig. 7, we show numerically that even for short sequence lengths, this upper bound is not loose.

Defining the estimation error as $\mathbf{e}_{\text{up}}^{\text{LSSE}} = \bar{\mathbf{c}} - \hat{\mathbf{c}}_{\text{up}}^{\text{LSSE}}$, the expected square error norm is obtained as

$$\begin{aligned} & \mathbb{E}_{\mathbf{r}, \bar{\mathbf{c}}}\{\|\mathbf{e}_{\text{up}}^{\text{LSSE}}\|^2\} \\ &= \mathbb{E}_{\mathbf{r}, \bar{\mathbf{c}}}\left\{\text{tr}\left\{\left(\bar{\mathbf{c}} - (\mathbf{S}^T \mathbf{S})^{-1} \mathbf{S}^T \mathbf{r}\right)\left(\bar{\mathbf{c}} - (\mathbf{S}^T \mathbf{S})^{-1} \mathbf{S}^T \mathbf{r}\right)^T\right\}\right\} \\ &= \mathbb{E}_{\mathbf{r}, \bar{\mathbf{c}}}\left\{\text{tr}\left\{\left(\mathbf{S}^T \mathbf{S}\right)^{-1} \mathbf{S}^T \mathbf{r} \mathbf{r}^T \mathbf{S}\left(\mathbf{S}^T \mathbf{S}\right)^{-1}\right\}\right. \\ & \quad \left.- 2\text{tr}\left\{\bar{\mathbf{c}} \mathbf{r}^T \mathbf{S}\left(\mathbf{S}^T \mathbf{S}\right)^{-1}\right\} + \text{tr}\left\{\bar{\mathbf{c}} \bar{\mathbf{c}}^T\right\}\right\}. \end{aligned} \quad (25)$$

Next, we calculate the expectation with respect to $(\mathbf{r}, \bar{\mathbf{c}})$ in (25) in two steps, namely first with respect to \mathbf{r} conditioned on $\bar{\mathbf{c}}$ and then with respect to $\bar{\mathbf{c}}$. Exploiting $\mathbb{E}_{\mathbf{X}}\{\text{tr}\{\mathbf{A}\mathbf{X}\mathbf{B}\}\} = \text{tr}\{\mathbf{A}\mathbb{E}_{\mathbf{X}}\{\mathbf{X}\}\mathbf{B}\}$ and $\mathbb{E}_{\mathbf{x}}\{\mathbf{x}\mathbf{x}^T\} = \boldsymbol{\lambda}\boldsymbol{\lambda}^T + \text{diag}\{\boldsymbol{\lambda}\}$, $\mathbb{E}\{\|\mathbf{e}_{\text{up}}^{\text{LSSE}}\|^2\}$ can be calculated as

$$\begin{aligned} & \mathbb{E}_{\bar{\mathbf{c}}}\mathbb{E}_{\mathbf{r}|\bar{\mathbf{c}}}\{\|\mathbf{e}_{\text{up}}^{\text{LSSE}}\|^2\} \\ &= \mathbb{E}_{\bar{\mathbf{c}}}\left\{\text{tr}\left\{\left(\mathbf{S}^T \mathbf{S}\right)^{-1} \mathbf{S}^T (\mathbf{S}\bar{\mathbf{c}}\bar{\mathbf{c}}^T \mathbf{S}^T) \mathbf{S}\left(\mathbf{S}^T \mathbf{S}\right)^{-1}\right\}\right. \\ & \quad \left.- 2\text{tr}\left\{\bar{\mathbf{c}} \bar{\mathbf{c}}^T \mathbf{S}^T \mathbf{S}\left(\mathbf{S}^T \mathbf{S}\right)^{-1}\right\} + \text{tr}\left\{\bar{\mathbf{c}} \bar{\mathbf{c}}^T\right\}\right. \\ & \quad \left.+ \text{tr}\left\{\left(\mathbf{S}^T \mathbf{S}\right)^{-1} \mathbf{S}^T \text{diag}\{\mathbf{S}\bar{\mathbf{c}}\} \mathbf{S}\left(\mathbf{S}^T \mathbf{S}\right)^{-1}\right\}\right\} \\ &= \mathbb{E}_{\bar{\mathbf{c}}}\left\{\text{tr}\left\{\mathbf{S}\left(\mathbf{S}^T \mathbf{S}\right)^{-2} \mathbf{S}^T \text{diag}\{\mathbf{S}\bar{\mathbf{c}}\}\right\}\right\} \\ &= \text{tr}\left\{\mathbf{S}^T \text{vdiag}\left\{\mathbf{S}\left(\mathbf{S}^T \mathbf{S}\right)^{-2} \mathbf{S}^T\right\} \boldsymbol{\mu}_{\bar{\mathbf{c}}}^T\right\}. \end{aligned} \quad (26)$$

Remark 11: From (26), we observe that the square error norm of $\bar{\mathbf{c}}$ for the LSSE estimator can be factorized into two terms, a first term $\mathbf{S}^T \text{vdiag}\left\{\mathbf{S}\left(\mathbf{S}^T \mathbf{S}\right)^{-2} \mathbf{S}^T\right\}$, which solely depends on the training sequence, multiplied by a second term $\boldsymbol{\mu}_{\bar{\mathbf{c}}}$, which depends on the MC channel. \square

The evaluation of the expression in (26) can be numerically challenging due to the required inversion of matrix $\mathbf{S}^T \mathbf{S}$, especially when one of the eigen-values of $\mathbf{S}^T \mathbf{S}$ is close to zero. One way to cope with this problem is to eliminate all sequences resulting in close-to-zero eigen-values for matrix $\mathbf{S}^T \mathbf{S}$ during the search. Formally, we can adopt the following search criterion for LSSE-based training sequence design

$$\mathbf{s}^{\text{LSSE}} = \underset{\mathbf{s} \in \tilde{\mathcal{S}}}{\text{argmin}} \text{tr}\left\{\mathbf{S}^T \text{vdiag}\left\{\mathbf{S}\left(\mathbf{S}^T \mathbf{S}\right)^{-2} \mathbf{S}^T\right\} \boldsymbol{\mu}_{\bar{\mathbf{c}}}^T\right\}, \quad (27)$$

where $\tilde{\mathcal{S}} = \{\mathbf{s} \in \mathcal{S}^K \mid |x| > \varepsilon, \forall x \in \text{eig}\{\mathbf{S}^T \mathbf{S}\}\}$ and ε is a small number which guarantees that the eigen-values of matrix $\mathbf{S}^T \mathbf{S}$ are not close to zero, e.g., in Section VI, we choose $\varepsilon = 10^{-9}$.

B. LMMSE-Based Training Sequence Design

Similar to the LSSE-based sequence design, the LMMSE estimate $\hat{\mathbf{c}}^{\text{MMSE}}$ in Lemma 3 can be used as the basis for sequence design. In this paper, we choose the optimal LMMSE-based training sequence such that the upper bound on the MMSE estimation error is minimized, i.e., $\mathbb{E}_{\mathbf{r}, \bar{\mathbf{c}}} \{ \|\mathbf{e}_{\text{up}}^{\text{MMSE}}\|^2 \}$ in (22). In particular, substituting \mathbf{F}^{MMSE} in (24) into (22), simplifying the resulting expression for $\mathbb{E}_{\mathbf{r}, \bar{\mathbf{c}}} \{ \|\mathbf{e}_{\text{up}}^{\text{MMSE}}\|^2 \}$, and removing the terms which do not depend on the sequence, we obtain the following criterion for the optimal LMMSE-based training sequence

$$\mathbf{s}^{\text{MMSE}} = \underset{\forall \mathbf{s} \in \mathcal{S}^K}{\text{argmax}} \text{tr} \left\{ \Phi_{\bar{\mathbf{c}}\bar{\mathbf{c}}}^T \mathbf{S}^T (\mathbf{S} \Phi_{\bar{\mathbf{c}}\bar{\mathbf{c}}} \mathbf{S}^T + \text{diag} \{ \mathbf{S} \boldsymbol{\mu}_{\bar{\mathbf{c}}} \})^{-1} \mathbf{S} \Phi_{\bar{\mathbf{c}}\bar{\mathbf{c}}} \right\} \quad (28)$$

We note that from (23a), we can conclude that matrix $\mathbf{S} \Phi_{\bar{\mathbf{c}}\bar{\mathbf{c}}} \mathbf{S}^T + \text{diag} \{ \mathbf{S} \boldsymbol{\mu}_{\bar{\mathbf{c}}} \}$ is a positive definite matrix, i.e., all eigen-values are positive.

Remark 12: We base our training sequence designs on the LSSE and LMMSE estimators (and not the ML and MAP estimators) because these two estimators lend themselves to elegant closed-form solutions for the estimated CIR which leads to relatively simpler criteria for training sequence design, cf. (27) and (28). In Section VI, we employ an exhaustive computer-based search to find the optimal LSSE-based and LMMSE-based training sequences by evaluating (27) and (28), respectively. We note that the complexity of the exhaustive search can be accommodated since the optimal training sequence is obtained offline and used for online CIR estimation. Nevertheless, to reduce the complexity of the exhaustive search, one can develop systematic approaches to solve the optimization problems in (27) and (28). This constitutes an interesting research problem which is beyond the scope of this paper and left for future work. \square

C. ISI-Free Training Sequence Design

One simple approach to estimate the CIR is to construct a training sequence such that ISI is avoided during estimation. In this case, in each symbol interval, the receiver will observe molecules which have been released by the transmitter in only one symbol interval and not in multiple symbol intervals. To this end, the transmitter releases N^{Tx} molecules every $L + 1$ symbol intervals and remains silent for the rest of the symbol intervals. This corresponds to the ON-OFF keying, i.e., $s[k] \in \{0, 1\}$, which is a special case of the general CSK modulation adopted in this paper. In particular, the sequence \mathbf{s} is constructed as follows:

$$s[k] = \begin{cases} 1, & \text{if } \frac{k-k_0}{L+1} \in \mathbb{Z} \\ 0, & \text{otherwise} \end{cases} \quad (29)$$

where $k \in \{1, \dots, K\}$, and k_0 is the index of the first symbol interval in which the transmitter releases molecules. Moreover, for this training sequence, the CIR can be straightforwardly estimated as

$$\hat{c}_l^{\text{ISIF}} = \frac{1}{|\mathcal{K}_l|} \left[\sum_{k \in \mathcal{K}_l} [r[k] - \hat{c}_n^{\text{ISIF}}] \right]^+, \quad l = 1, \dots, L \quad (30a)$$

$$\hat{c}_n^{\text{ISIF}} = \frac{1}{|\mathcal{K}_n|} \sum_{k \in \mathcal{K}_n} r[k], \quad (30b)$$

where $\mathcal{K}_l = \{k | \frac{k-k_0-L+1}{L+1} \in \mathbb{Z} \wedge k \in \{1, \dots, K\}\}$, $\mathcal{K}_n = \{k | \frac{k-k_0-L}{L+1} \in \mathbb{Z} \wedge k \in \{1, \dots, K\}\}$, and $[\cdot]^+$ is needed to ensure that all estimated channel taps are non-negative, i.e., $\hat{\mathbf{c}}^{\text{ISIF}} \geq \mathbf{0}$ holds.

Remark 13: The ISI-free training sequence in (29) permits the use of the simple estimator in (30). Thereby, the mathematical calculation for \hat{c}_n^{ISIF} boils down to averaging over those elements of the observation vector \mathbf{r} which are only affected by the external noise. Similarly, the computation of \hat{c}_l^{ISIF} basically reduces to averaging over those elements of \mathbf{r} which are affected by \bar{c}_l and the impact of the estimated mean of the external noise \hat{c}_n^{ISIF} is removed. The ISI-free training sequence (29) and the corresponding simple estimator in (30) are suitable options for applications where nanoreceivers with low computational capability have to be employed for CIR estimation. We note that, for the ISI-free training sequence in (29), the asymptotic solutions of the ML, LSSE, MAP, and LMMSE estimates as $K \rightarrow \infty$ reduce to the estimate given in (30), i.e., $\hat{\mathbf{c}}^{\text{ML}} = \hat{\mathbf{c}}^{\text{LSSE}} = \hat{\mathbf{c}}^{\text{MAP}} = \hat{\mathbf{c}}^{\text{MMSE}} = \hat{\mathbf{c}}^{\text{ISIF}}$. \square

VI. PERFORMANCE EVALUATION

In this section, we evaluate the performances of the different estimation techniques and training sequence designs developed in this paper for ON-OFF keying signaling, i.e., $s[k] \in \{0, 1\}$. For simplicity, for the results provided in this section, we generate CIR $\bar{\mathbf{c}}$ based on (1) and (2). However, we emphasize that the proposed estimation framework is not limited to the particular channel and receiver models assumed in (1) and (2). We use (1) and (2) only to obtain a CIR $\bar{\mathbf{c}}$ which is representative of a typical CIR in MC. In particular, we assume a point source with impulsive molecule release and $N^{\text{Tx}} = 10^5$, a fully transparent spherical receiver with radius 50 nm, and an unbounded environment with $D = 4.365 \times 10^{-10} \frac{\text{m}^2}{\text{s}}$ [13]. The distance between the transmitter and the receiver is assumed to be $|\mathbf{a}| = 400$ nm. The receiver counts the number of molecules once per symbol interval at time $T_{\text{smp}} = \text{argmax}_t \bar{C}(\mathbf{a}, t)$ after the beginning of the symbol interval where $\bar{C}(\mathbf{a}, t)$ is computed based on (2). The noise mean is chosen as $\bar{c}_n = 0.2 \text{max}_t \bar{C}(\mathbf{a}, t)$. Furthermore, the symbol duration and the number of taps L are chosen such that $\bar{c}_{L+1} < 0.05 \bar{c}_1$. Based on the aforementioned assumptions, we obtain a typical/default value for the CIR vector which is denoted by $\bar{\mathbf{c}}^{\text{def}}$, e.g., $\bar{\mathbf{c}}^{\text{def}} = [60.22, 11.76, 5.13, 12.04]^T$ for $L = 3$. In practice, however, there may be random variations in the underlying channel parameters, e.g., D , $|\mathbf{a}|$, N^{Tx} , which leads to random variations in the CIR. To take this into account, we assume that the CIR vector in each estimation block is a realization of a RV according to $\bar{\mathbf{c}} = [\bar{\mathbf{c}}^{\text{Gaus}}]^+ = [\bar{\mathbf{c}}^{\text{def}} + \sigma \text{diag}\{\bar{\mathbf{c}}^{\text{def}}\} \mathcal{N}(\mathbf{0}, \mathbf{I})]^+$, where σ is the standard deviation of RV $\bar{\mathbf{c}}^{\text{Gaus}}$, see Remark 8 for further discussion. We note that as $\sigma \rightarrow 0$, the MC channel becomes deterministic, and for large σ , the MC channel is highly stochastic.

For the results reported in Figs. 3-6, the training sequences are constructed by concatenating n copies of the binary sequence [1100100101] of length 10, i.e., $K = 10n$. Moreover, the results reported in Figs. 3-6 are Monte Carlo simulations where each point of the curves is obtained by averaging over

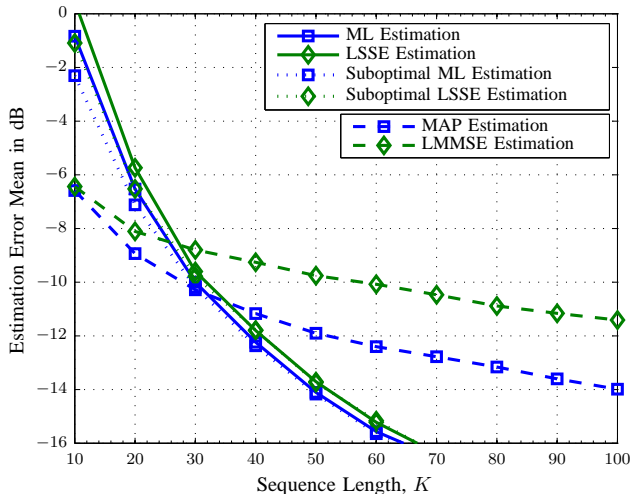


Fig. 3. Norm of the estimation error mean, $\|\mathbb{E}\{\mathbf{e}\}\|$, in dB vs. the training sequence length, K , for $L = 3$ and $\sigma^2 = 0.1$.

10^5 random realizations of observation vector \mathbf{r} and $\bar{\mathbf{c}}$. In the following, in Figs. 3 and 4, we present results for $L = 3$ and $\sigma^2 = 0.1$. In particular, in Fig. 3, we show the norm of the mean of the estimation error, $\|\mathbb{E}\{\mathbf{e}\}\|$, where $\mathbf{e} = \hat{\mathbf{c}} - \bar{\mathbf{c}}$, in dB vs. the training sequence length, K . Since for a given $\bar{\mathbf{c}}$, $\mathbb{E}_{\mathbf{r}|\bar{\mathbf{c}}}\{\mathbf{e}\} = \mathbb{E}_{\mathbf{r}|\bar{\mathbf{c}}}\{\hat{\mathbf{c}}\} - \bar{\mathbf{c}}$ holds, $\|\mathbb{E}\{\mathbf{e}\}\| = \|\mathbb{E}_{\bar{\mathbf{c}}}\mathbb{E}_{\mathbf{r}|\bar{\mathbf{c}}}\{\mathbf{e}\}\|$ is a measure for the *average* bias of the estimate $\hat{\mathbf{c}}$. We observe from Fig. 3 that the mean of the estimation error decreases as the sequence length increases. Therefore, the proposed estimators are biased for short sequence lengths, but as the sequence length increases, they become asymptotically unbiased, i.e., $\mathbb{E}\{\hat{\mathbf{c}}\} \rightarrow \bar{\mathbf{c}}$ as $K \rightarrow \infty$, cf. Corollary 1 and Remarks 3, 6, and 10.

In Fig. 4, we show the estimation error variance⁵, $\mathbb{E}\{\|\mathbf{e} - \mathbb{E}\{\mathbf{e}\}\|^2\}$, in dB vs. the training sequence length, K . As expected, the variance of the estimation error decreases with increasing training sequence length. For CIR estimation without statistical channel knowledge, we observe in Fig. 4 that the gap between the error variances of the suboptimal ML-based (LSSE-based) estimate and the optimal ML (LSSE) estimate is small for short sequence lengths and vanishes as $K \rightarrow \infty$. Furthermore, for the considered set of parameters, the ML estimator outperforms the LSSE estimator by a margin of less than 1 dB. These results suggest that the simple LSSE estimator provides a favorable complexity-performance tradeoff for CIR estimation in the considered MC system. For CIR estimation with statistical channel knowledge, we observe from Fig. 4 that the error variance of the LMMSE estimate is slightly higher than that of the MAP estimate which reveals the effectiveness of the proposed LMMSE estimator. Additionally, for short sequence lengths, a reduction of up to 5 dB in the estimation error variance is attainable with the MAP/LMMSE

⁵We note that the estimation error variance *normalized* to $\|\mathbb{E}\{\bar{\mathbf{c}}\}\|^2$ yields very small values. For instance, in Fig. 4, the value of the normalized estimation error variance is approximately 36 dB less than the value of the estimation error variance.

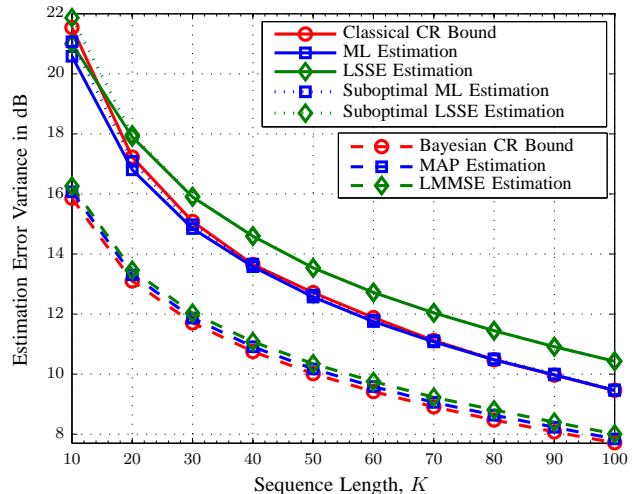


Fig. 4. Estimation error variance, $\mathbb{E}\{\|\mathbf{e} - \mathbb{E}\{\mathbf{e}\}\|^2\}$, in dB vs. the training sequence length, K , for $L = 3$ and $\sigma^2 = 0.1$.

estimators as compared to the ML/LSSE estimators at the cost of the required acquisition of statistical channel knowledge. However, this gain vanishes as $K \rightarrow \infty$. Finally, we note that for short sequence lengths, the variances of the proposed estimators can even be lower than the corresponding classical/Bayesian CR bound as these estimators are biased and the CR bound is a valid lower bound only for unbiased estimators, see Fig. 3. However, as K increases, all estimators become asymptotically unbiased, see Fig. 3. Fig. 4 shows that, for large K , the error variance of the ML estimator coincides with the classical CR bound and the error variance of the MAP estimator is very close to the Bayesian CR bound.

To further study the performance of the proposed estimators, in Figs. 5 and 6, we show results only for the suboptimal LSSE estimator and the LMMSE estimator. Note that these linear estimators are easier to implement compared to the other proposed estimators. In Fig. 5, we show the estimation error variance, $\mathbb{E}\{\|\mathbf{e} - \mathbb{E}\{\mathbf{e}\}\|^2\}$, in dB vs. the training sequence length, K for $L = 3$ and $\sigma^2 \in \{1, 0.5, 0.1, 0.05, 0.01\}$. As expected, the error variance of the LMMSE estimator decreases as σ^2 decreases. In particular, when $\sigma^2 \rightarrow \infty$, the statistical channel knowledge becomes useless and when $\sigma^2 \rightarrow 0$, the first order statistics $\boldsymbol{\mu}_{\bar{\mathbf{c}}}$ become a perfectly precise estimate of $\bar{\mathbf{c}}$. Thereby, depending on the values of K and σ^2 , we observe from Fig. 5 that the LMMSE estimator achieves gains of 1-9 dB compared to the LSSE estimator at the expense of requiring knowledge of the first and second order statistics of the CIR. Moreover, as suggested by (26), the LSSE error variance depends only on $\boldsymbol{\mu}_{\bar{\mathbf{c}}}$ which is approximately constant for all curves in Fig. 5. In particular, the small change in the LSSE error variance in Fig. 5 is due to the fact that although by increasing σ^2 , the mean of $\bar{\mathbf{c}}^{\text{Gaus}}$ remains unchanged, the mean of $\bar{\mathbf{c}} = [\bar{\mathbf{c}}^{\text{Gaus}}]^+$ changes since the instances, in which the elements of $\bar{\mathbf{c}}^{\text{Gaus}}$ are negative, occur more frequently.

In order to compare the performances of the considered estimators for different numbers of channel memory taps, L ,

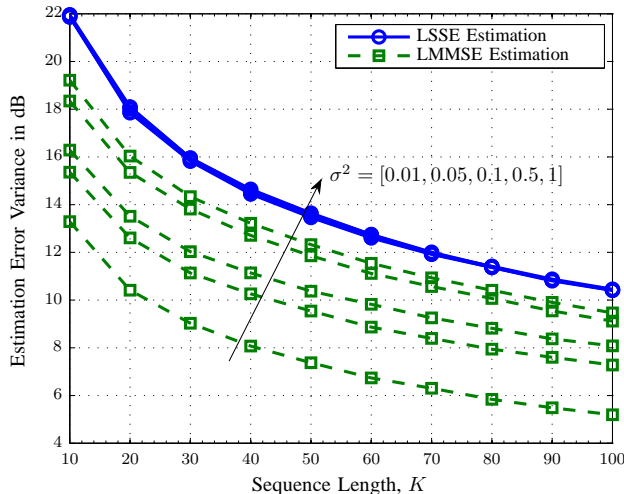


Fig. 5. Estimation error variance, $\mathbb{E} \left\{ \|\mathbf{e} - \mathbb{E} \{\mathbf{e}\}\|^2 \right\}$, in dB vs. the training sequence length, K , for $L = 3$ and $\sigma^2 = [0.01, 0.05, 0.1, 0.5, 1]$.

we define the normalized variance of the estimation error as

$$\overline{\text{Var}}_e = \frac{\mathbb{E} \left\{ \|\mathbf{e}\|^2 \right\} - \|\mathbb{E} \{\mathbf{e}\}\|^2}{\|\mathbb{E} \{\bar{\mathbf{c}}\}\|^2}. \quad (31)$$

In Fig. 6, we show the normalized estimation error variance, $\overline{\text{Var}}_e$, in dB vs. the training sequence length, K , for $L \in \{1, 2, 3, 4, 5\}$ and $\sigma^2 = 0.1$. Thereby, we observe that the error variance increases as the number of memory taps increases. This is due to the fact that as L increases, the number of unknown parameters which have to be estimated increases. Furthermore, Fig. 6 shows that the gap between the error variances of the LMMSE and LSSE estimators increases as L increases.

Next, we investigate the performances of the optimal LSSE-/LMMSE-based and ISI-free training sequence designs developed in Section V. Here, we employ a computer-based search to find the optimal sequences based on the LSSE-based criterion in (27) where $\varepsilon = 10^{-9}$ and the LMMSE-based criterion in (28). We consider short sequence lengths, i.e., $K \leq 20$, due to the exponential increase of the computational complexity of the exhaustive search with respect to the sequence length. Moreover, since there are $L + 1$ unknown parameters, we require at least $L + 1$ observations for estimation, i.e., $K - L + 1 \geq L + 1$ or equivalently $K \geq 2L$. In Table I, we present the optimal sequences obtained for $L \in \{1, 3, 5\}$, $K \in \{10, 20\}$, and $\sigma^2 = 0.1$. We note that the optimal sequences which are obtained from (27) and (28) are not unique and only one of the optimal sequences is shown in Table I for each value of K and L . The optimal sequence shown in red font in Table I is an ISI-free sequence as defined in (29).

In Fig. 7, we show the normalized LSSE estimation error variance, $\overline{\text{Var}}_e$, in dB vs. the training sequence length, K , for $L \in \{1, 2, 3, 4, 5\}$ and $\sigma^2 = 0.1$. Thereby, we report the analytical results for the upper bound in (26) and Monte Carlo simulation results for 10^5 random realizations of \mathbf{r} and

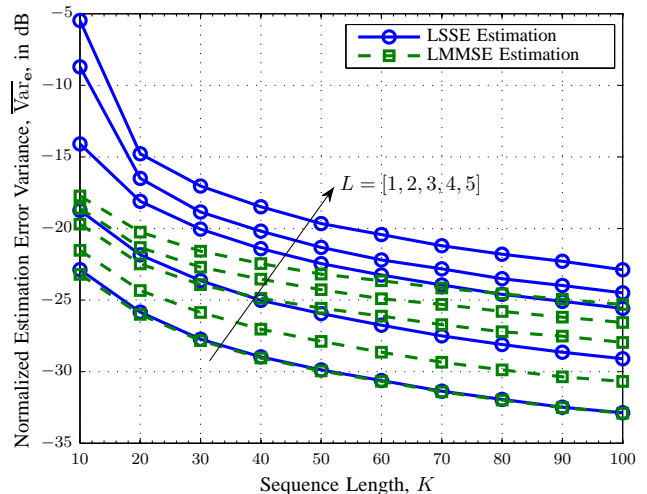


Fig. 6. Normalized estimation error variance, $\overline{\text{Var}}_e$, in dB vs. the training sequence length, K , for $L \in \{1, 2, 3, 4, 5\}$ and $\sigma^2 = 0.1$.

$\bar{\mathbf{c}}$. For the ISI-free sequence, we also report the performance of the simple estimation method in (30) in addition to the performance of LSSE estimation. Fig. 7 confirms that (26) is a tight upper bound even for short sequence lengths. Moreover, we observe from Fig. 7 that the difference between the error variances of the ISI-free sequence and the optimal sequence increases as L increases. This result suggests that for MC channels with small numbers of taps, a simple ISI-free training sequence is a suitable option. Furthermore, as expected, the estimation error decreases with increasing training sequence length and increases with increasing number of CIR coefficients.

In Fig. 8, we show the normalized LMMSE estimation error, $\overline{\text{Var}}_e$, in dB vs. the training sequence length, K , for $L \in \{1, 3, 5\}$ and $\sigma^2 = 0.1$. In general, we can observe a similar behavior as in Fig. 7, hence, we highlight only the differences. In particular, the simulation results for LMMSE estimation and the corresponding upper bound in (22) coincide which reveals that the effect of the instances for which the elements of $\mathbf{F}^{\text{MMSE}} \mathbf{r}$ are negative is negligible and hence $\hat{\mathbf{c}}^{\text{MMSE}} = [\mathbf{F}^{\text{MMSE}} \mathbf{r}]^+ \approx \mathbf{F}^{\text{MMSE}} \mathbf{r}$. Moreover, for $L = 3$ and $L = 5$, there is a considerable gap between the variances of the MMSE estimators for the optimal LMMSE-based training sequence and the ISI-free sequence.

VII. CONCLUSIONS

In this paper, we developed a training-based CIR estimation framework which enables the acquisition of the CIR based on the observed number of molecules at the receiver due to emission of a sequence of known numbers of molecules by the transmitter. In particular, for the case when statistical channel knowledge is not available, we derived the optimal ML estimator, the suboptimal LSSE estimator, and the classical CR lower bound. On the other hand, for the case when knowledge of the channel statistics is available, we provided the optimal MAP estimator, the suboptimal LMMSE estimator, and the

TABLE I
EXAMPLES OF OPTIMAL LSSE/LMMSE SEQUENCES OBTAINED BY A COMPUTER-BASED SEARCH
FOR $L \in \{1, 3, 5\}$, $K \in \{10, 20\}$, AND $\sigma^2 = 0.1$.

	Criterion	$K = 10$	$K = 20$
$L = 1$	LSSE-based	$\mathbf{s}^* = [1001101110]^T$	$\mathbf{s}^* = [00101110111010101111]^T$
	LMMSE-based	$\mathbf{s}^* = [1111000111]^T$	$\mathbf{s}^* = [11011110101100010111]^T$
$L = 3$	LSSE-based	$\mathbf{s}^* = [1100001001]^T$	$\mathbf{s}^* = [10101101101101100000]^T$
	LMMSE-based	$\mathbf{s}^* = [0001101011]^T$	$\mathbf{s}^* = [00110101100000111011]^T$
$L = 5$	LSSE-based	$\mathbf{s}^* = [1000001000]^T$	$\mathbf{s}^* = [11111110000100001000]^T$
	LMMSE-based	$\mathbf{s}^* = [0000010110]^T$	$\mathbf{s}^* = [0000001100101010100111]^T$

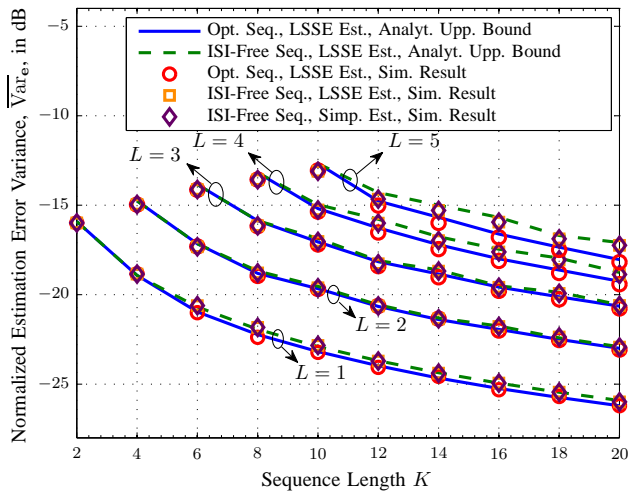


Fig. 7. Normalized LSSE estimation error variance, $\overline{\text{Var}}_e$, in dB vs. the training sequence length, K , for $L \in \{1, 2, 3, 4, 5\}$ and $\sigma^2 = 0.1$.

Bayesian CR lower bound. Furthermore, we studied optimal LSSE-/LMMSE-based and suboptimal training sequence designs for the considered MC system. Our simulation results revealed that the simple LSSE and LMMSE estimators provide favorable tradeoffs between complexity and performance. Additionally, for LSSE estimation, the proposed simple ISI-free sequences achieve a similar performance as the optimal sequences whereas, for LMMSE estimation, the performance gap between the ISI-free and the optimal sequences is not negligible specially for larger numbers of channel memory taps.

In this paper, we investigated the performance of the proposed CIR estimators and training sequences in terms of the estimation error variance. Studying the effect of the quality of the CIR estimates on the end-to-end bit error rate performance of MC systems is an interesting and important direction for future research.

APPENDIX A PROOF OF LEMMA 1

The problem in (12) is a convex optimization problem in variable $\bar{\mathbf{c}}$ because $g(\bar{\mathbf{c}})$ is a concave function in $\bar{\mathbf{c}}$ and the feasible set $\bar{\mathbf{c}} \geq \mathbf{0}$ is linear in $\bar{\mathbf{c}}$. In particular, $\ln(\bar{\mathbf{c}}^T \mathbf{s}_k)$ is concave since $\bar{\mathbf{c}}^T \mathbf{s}_k$ is affine and the log-function is concave [36, Chapter 3]. Therefore, $g(\bar{\mathbf{c}})$ is a sum of weighted concave

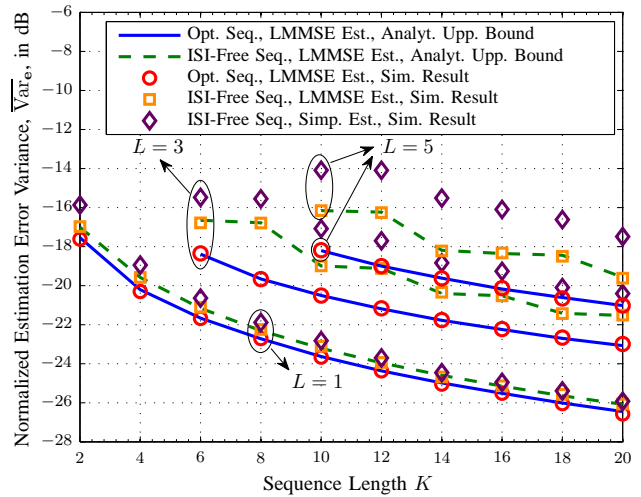


Fig. 8. Normalized LMMSE estimation error variance, $\overline{\text{Var}}_e$, in dB vs. the training sequence length, K , for $L \in \{1, 3, 5\}$ and $\sigma^2 = 0.1$.

terms $r[k] \ln(\bar{\mathbf{c}}^T \mathbf{s}_k)$ and affine terms $\bar{\mathbf{c}}^T \mathbf{s}_k$ which in turn yields a concave function [36, Chapter 3]. For the constrained convex problem in (12), the optimal solution falls into one of the following two categories:

Stationary Point: In this case, the optimal solution is found by taking the derivative of $g(\bar{\mathbf{c}})$ with respect to $\bar{\mathbf{c}}$ which is given in (13) for $\mathcal{A}_n = \mathcal{F}$ where $\bar{\mathbf{c}}^{\mathcal{F}} = \bar{\mathbf{c}}$ and $\mathbf{s}_k^{\mathcal{F}} = \mathbf{s}_k$ hold. Note that this stationary point is the global optimal solution of the unconstrained version of the problem in (12), i.e., when constraint $\bar{\mathbf{c}} \geq \mathbf{0}$ is dropped. Therefore, if $\bar{\mathbf{c}}^{\mathcal{F}}$ falls into the feasible set, i.e., $\bar{\mathbf{c}}^{\mathcal{F}} \geq \mathbf{0}$ holds, it is also the optimal solution of the constrained problem in (12) and hence, we obtain $\hat{\mathbf{c}}^{\text{ML}} = \bar{\mathbf{c}}^{\mathcal{F}}$.

Boundary Point: In this case, for the optimal solution, some of the elements of $\hat{\mathbf{c}}$ are zero. Since it is not a priori known which elements are zero, we have to consider all possible cases. To do so, we use auxiliary variables $\bar{\mathbf{c}}^{\mathcal{A}_n}$ and $\mathbf{s}_k^{\mathcal{A}_n}$ where set \mathcal{A}_n specifies the indices of the non-zero elements of $\bar{\mathbf{c}}$. For a given \mathcal{A}_n , we formulate a new problem by substituting $\bar{\mathbf{c}}^{\mathcal{A}_n}$ and $\mathbf{s}_k^{\mathcal{A}_n}$ for $\bar{\mathbf{c}}$ and \mathbf{s}_k in (12), respectively. The stationary point of the new problem can be found by taking the derivative of $g(\bar{\mathbf{c}}^{\mathcal{A}_n})$ with respect to $\bar{\mathbf{c}}^{\mathcal{A}_n}$ which is given in (13). Here, if $\bar{\mathbf{c}}^{\mathcal{A}_n} \geq \mathbf{0}$ does not hold, we discard $\bar{\mathbf{c}}^{\mathcal{A}_n}$, otherwise, it is a candidate for the optimal solution. Therefore, we construct the candidate ML CIR estimate, denoted by $\hat{\mathbf{c}}^{\text{CAN}}$, such that

the elements of $\hat{\mathbf{c}}^{\text{CAN}}$ whose indices are in \mathcal{A}_n are equal to the values of the corresponding elements in $\bar{\mathbf{c}}^{\mathcal{A}_n}$ and the remaining elements are equal to zero. The resulting $\hat{\mathbf{c}}^{\text{CAN}}$ is saved in the candidate set \mathcal{C} . Finally, the ML estimate, $\hat{\mathbf{c}}^{\text{ML}}$, is given by that $\hat{\mathbf{c}}^{\text{CAN}}$ in set \mathcal{C} which maximizes $g(\bar{\mathbf{c}})$.

The above results are concisely summarized in Algorithm 1 which concludes the proof.

APPENDIX B PROOF OF LEMMA 2

The optimization problem in (15) is convex since $\|\epsilon\|^2$ is quadratic in variable $\bar{\mathbf{c}}$, $\mathbf{S}^T \mathbf{S} \succeq 0$ holds, and the feasible set $\bar{\mathbf{c}} \geq \mathbf{0}$ is linear in $\bar{\mathbf{c}}$ [36, Chapter 4]. The constrained convex problem in (15) can be solved using a similar methodology as was used for finding the ML estimate in Lemma 1. Hence, in order to avoid repetition and due to the space constraint, we provide only a sketch of the proof for Lemma 2 in the following. In particular, the optimal LSSE estimate is either a stationary point or a boundary point for the problem in (15). Moreover, if the solution is a boundary point for the original problem in (15), we can formulate a new problem by substituting $\bar{\mathbf{c}}^{\mathcal{A}_n}$ and $\mathbf{s}_k^{\mathcal{A}_n}$ for $\bar{\mathbf{c}}$ and \mathbf{s}_k in (15), respectively, where the solution of the new problem has to be a stationary point, see the proof of Lemma 1. For a given \mathcal{A}_n , the derivative of $\|\epsilon^{\mathcal{A}_n}\|^2$, where $\epsilon^{\mathcal{A}_n} = \mathbf{r} - \mathbf{S}^{\mathcal{A}_n} \bar{\mathbf{c}}^{\mathcal{A}_n}$, with respect to $\bar{\mathbf{c}}^{\mathcal{A}_n}$ is obtained as

$$\frac{\partial \|\epsilon^{\mathcal{A}_n}\|^2}{\partial \bar{\mathbf{c}}^{\mathcal{A}_n}} = 2(\mathbf{S}^{\mathcal{A}_n})^T \mathbf{S}^{\mathcal{A}_n} \bar{\mathbf{c}}^{\mathcal{A}_n} - 2(\mathbf{S}^{\mathcal{A}_n})^T \mathbf{r} \stackrel{!}{=} 0, \quad (32)$$

where we employed the vector differentiation rules $\frac{\partial \text{tr}\{\mathbf{A}\mathbf{x}\mathbf{x}^T\}}{\partial \mathbf{x}} = (\mathbf{A} + \mathbf{A}^T) \mathbf{x}$ and $\frac{\partial \text{tr}\{\mathbf{A}\mathbf{x}\}}{\partial \mathbf{x}} = \mathbf{A}^T$ [35, Table I]. Solving (32) leads to (17). Now, we first find the stationary point of the original problem by substituting $\mathcal{A}_n = \mathcal{F}$ in (17). If $\bar{\mathbf{c}}^{\mathcal{F}} \geq \mathbf{0}$ holds, $\bar{\mathbf{c}}^{\mathcal{F}}$ is the optimal LSSE estimate, otherwise, we have to calculate $\bar{\mathbf{c}}^{\mathcal{A}_n}$ for all possible boundary points, i.e., all elements of \mathcal{A}_n . Among all $\bar{\mathbf{c}}^{\mathcal{A}_n}$ for which $\bar{\mathbf{c}}^{\mathcal{A}_n} \geq \mathbf{0}$ holds, the LSSE estimate is the one which minimizes $\|\epsilon\|^2$. These results are summarized in Algorithm 1 which concludes the proof.

APPENDIX C PROOF OF COROLLARY 1

To show that the LSSE estimator is biased in general, we neglect the constraint that $\bar{\mathbf{c}} \geq \mathbf{0}$ has to hold in (15) which yields an upper bound on the estimation error for the LSSE estimator, denoted by $\hat{\mathbf{c}}_{\text{up}}^{\text{LSSE}} = (\mathbf{S}^T \mathbf{S})^{-1} \mathbf{S}^T \mathbf{r}$. Thereby, we first show that $\hat{\mathbf{c}}_{\text{up}}^{\text{LSSE}}$ is unbiased. The unbiasedness of $\hat{\mathbf{c}}_{\text{up}}^{\text{LSSE}}$ is easily shown as

$$\begin{aligned} \mathbb{E}_{\mathbf{r}|\bar{\mathbf{c}}} \{\hat{\mathbf{c}}_{\text{up}}^{\text{LSSE}}\} &= \mathbb{E}_{\mathbf{r}|\bar{\mathbf{c}}} \left\{ (\mathbf{S}^T \mathbf{S})^{-1} \mathbf{S}^T \mathbf{r} \right\} = (\mathbf{S}^T \mathbf{S})^{-1} \mathbf{S}^T \mathbb{E}_{\mathbf{r}|\bar{\mathbf{c}}} \{\mathbf{r}\} \\ &= (\mathbf{S}^T \mathbf{S})^{-1} \mathbf{S}^T \mathbf{S} \bar{\mathbf{c}} = \bar{\mathbf{c}}. \end{aligned} \quad (33)$$

For the case when $\hat{\mathbf{c}}_{\text{up}}^{\text{LSSE}} \geq \mathbf{0}$ holds, the original $\hat{\mathbf{c}}^{\text{LSSE}}$ is identical to $\hat{\mathbf{c}}_{\text{up}}^{\text{LSSE}}$. Otherwise, for the case when some of the elements of $\hat{\mathbf{c}}_{\text{up}}^{\text{LSSE}}$ are negative, $\hat{\mathbf{c}}^{\text{LSSE}}$ deviates from $\hat{\mathbf{c}}_{\text{up}}^{\text{LSSE}}$ to ensure that $\hat{\mathbf{c}}^{\text{LSSE}} \geq \mathbf{0}$ holds. Therefore, the elements of $\mathbb{E}_{\mathbf{r}|\bar{\mathbf{c}}} \{\hat{\mathbf{c}}^{\text{LSSE}}\}$ have a positive bias compared to their respective elements in

$\mathbb{E}_{\mathbf{r}|\bar{\mathbf{c}}} \{\hat{\mathbf{c}}_{\text{up}}^{\text{LSSE}}\}$ which indicates that the LSSE estimate, $\hat{\mathbf{c}}^{\text{LSSE}}$, is biased.

To show that the LSSE estimator becomes asymptotically unbiased, as $K \rightarrow \infty$, we first prove that $\hat{\mathbf{c}}_{\text{up}}^{\text{LSSE}}$ is a consistent estimator, i.e., $\hat{\mathbf{c}}_{\text{up}}^{\text{LSSE}} \rightarrow \bar{\mathbf{c}}$ as $K \rightarrow \infty$. Here, since $\hat{\mathbf{c}}_{\text{up}}^{\text{LSSE}}$ provides an upper bound on the estimation error of $\hat{\mathbf{c}}^{\text{LSSE}}$, we can conclude that if $\hat{\mathbf{c}}_{\text{up}}^{\text{LSSE}}$ is consistent, then $\hat{\mathbf{c}}^{\text{LSSE}}$ is also consistent. In other words, as $K \rightarrow \infty$, we obtain $\hat{\mathbf{c}}^{\text{LSSE}} \rightarrow \hat{\mathbf{c}}_{\text{up}}^{\text{LSSE}} \rightarrow \bar{\mathbf{c}}$ and hence, the asymptotic unbiasedness of the LSSE estimator.

In the following, we employ a well-known approach which is based on the law of large numbers (LLN) to show the consistency of $\hat{\mathbf{c}}_{\text{up}}^{\text{LSSE}}$ [37], [38]. To apply the LLN, we rewrite $\mathbf{S} = [\mathbf{l}_1, \mathbf{l}_2, \dots, \mathbf{l}_L, \mathbf{l}_n]$ where \mathbf{l}_l , $l \in \{1, 2, \dots, L, n\}$, are the columns of \mathbf{S} . We note that for each element of vector $\mathbf{S}^T \mathbf{r} = [\mathbf{l}_1^T \mathbf{r}, \mathbf{l}_2^T \mathbf{r}, \dots, \mathbf{l}_L^T \mathbf{r}, \mathbf{l}_n^T \mathbf{r}]$, we have a deterministic term \mathbf{l}_l , $l \in \{1, 2, \dots, L, n\}$ and a stochastic term \mathbf{r} . Therefore, using the LLN, we obtain $\frac{1}{K-L+1} \mathbf{l}_l^T \mathbf{r} \xrightarrow{K \rightarrow \infty} \frac{1}{K-L+1} \mathbf{l}_l^T \mathbf{S} \bar{\mathbf{c}}$. Here, we emphasize that $\frac{1}{K-L+1} \mathbf{l}_l^T \mathbf{r} \xrightarrow{K \rightarrow \infty} \frac{1}{K-L+1} \mathbf{l}_l^T \mathbf{S} \bar{\mathbf{c}}$ does not hold. However, $\frac{1}{K-L+1} \mathbf{l}_l^T \mathbf{r}$ is indeed an averaging over all observations in which the element \bar{c}_l is present based on (3). Substituting these results into $\hat{\mathbf{c}}_{\text{up}}^{\text{LSSE}}$, we obtain

$$\hat{\mathbf{c}}_{\text{up}}^{\text{LSSE}} = (\mathbf{S}^T \mathbf{S})^{-1} \mathbf{S}^T \mathbf{r} \xrightarrow{K \rightarrow \infty} (\mathbf{S}^T \mathbf{S})^{-1} \mathbf{S}^T \mathbf{S} \bar{\mathbf{c}} = \bar{\mathbf{c}}. \quad (34)$$

Since $\hat{\mathbf{c}}_{\text{up}}^{\text{LSSE}}$ is a consistent estimator and also provides an upper bound on the estimation error for $\hat{\mathbf{c}}^{\text{LSSE}}$, we can conclude that $\hat{\mathbf{c}}^{\text{LSSE}}$ is a consistent estimator, too. This completes the proof.

APPENDIX D PROOF OF LEMMA 3

The optimization problem in (21) is a convex optimization problem since the cost function is quadratic in \mathbf{F} [36]. Moreover, since the feasible set of \mathbf{F} is not constrained, the global optimal \mathbf{F} has to be a stationary point which can be found by equating the derivative of $\mathbb{E}_{\mathbf{r}, \bar{\mathbf{c}}} \{\|\mathbf{e}_{\text{up}}^{\text{MMSE}}\|^2\}$ with respect to \mathbf{F} to zero, i.e.,

$$\begin{aligned} \frac{\partial \mathbb{E}_{\mathbf{r}, \bar{\mathbf{c}}} \{\|\mathbf{e}_{\text{up}}^{\text{MMSE}}\|^2\}}{\partial \mathbf{F}} &= \mathbf{F} (\Phi_{\mathbf{r}\mathbf{r}} + \Phi_{\mathbf{r}\mathbf{r}}^T) - 2\Phi_{\mathbf{r}\bar{\mathbf{c}}}^T \\ &= 2\mathbf{F} (\mathbf{S}\Phi_{\bar{\mathbf{c}}\bar{\mathbf{c}}}\mathbf{S}^T + \text{diag}\{\mathbf{S}\boldsymbol{\mu}_{\bar{\mathbf{c}}}\}) - 2\Phi_{\bar{\mathbf{c}}\bar{\mathbf{c}}}^T \mathbf{S}^T \stackrel{!}{=} \mathbf{0}. \end{aligned} \quad (35)$$

Solving the above linear equation leads to (24) and concludes the proof.

REFERENCES

- [1] T. Nakano, M. Moore, F. Wei, A. Vasilakos, and J. Shuai, "Molecular Communication and Networking: Opportunities and Challenges," *IEEE Trans. NanoBiosci.*, vol. 11, no. 2, pp. 135–148, Jun. 2012.
- [2] N. Farsad, H. Yilmaz, A. Eckford, C. Chae, and W. Guo, "A Comprehensive Survey of Recent Advancements in Molecular Communication," *IEEE Commun. Surveys Tutorials*, vol. PP, no. 99, pp. 1–1, 2016.
- [3] I. Akyildiz, F. Brunetti, and C. Blazquez, "Nanonetworks: A New Communication Paradigm," *Comput. Net.*, vol. 52, pp. 2260–2279, Apr. 2008.
- [4] B. Alberts, D. Bray, K. Hopkin, A. Johnson, J. Lewis, M. Raff, K. Roberts, and P. Walter, *Essential Cell Biology*. Garland Science, 4th ed., 2014.

- [5] A. Noel, K. Cheung, and R. Schober, "Optimal Receiver Design for Diffusive Molecular Communication with Flow and Additive Noise," *IEEE Trans. NanoBiosci.*, vol. 13, no. 3, pp. 350–362, Sept. 2014.
- [6] M. Mahfuz, D. Makrakis, and H. Moutfah, "A Comprehensive Study of Sampling-Based Optimum Signal Detection in Concentration-Encoded Molecular Communication," *IEEE Trans. NanoBiosci.*, vol. 13, no. 3, pp. 208–222, Sept. 2014.
- [7] A. Akkaya, H. Yilmaz, C. Chae, and T. Tugcu, "Effect of Receptor Density and Size on Signal Reception in Molecular Communication via Diffusion With an Absorbing Receiver," *IEEE Commun. Lett.*, vol. 19, no. 2, pp. 155–158, Feb. 2015.
- [8] A. Ahmadzadeh, H. Arjmandi, A. Burkovski, and R. Schober, "Reactive Receiver Modeling for Diffusive Molecular Communication Systems with Molecule Degradation," in *Proc. IEEE ICC*, Kuala Lumpur, May 2016, pp. 1–7.
- [9] H. Yilmaz, A. Heren, T. Tugcu, and C. B. Chae, "Three-Dimensional Channel Characteristics for Molecular Communications With an Absorbing Receiver," *IEEE Commun. Lett.*, vol. 18, no. 6, pp. 929–932, Jun. 2014.
- [10] G. Wei and R. Marculescu, "Miniature Devices in the Wild: Modeling Molecular Communication in Complex Extracellular Spaces," *IEEE J. Select. Areas Commun.*, vol. 32, no. 12, pp. 2344–2353, Dec. 2014.
- [11] M. Moore, T. Nakano, A. Enomoto, and T. Suda, "Measuring Distance From Single Spike Feedback Signals in Molecular Communication," *IEEE Trans. Sig. Process.*, vol. 60, no. 7, pp. 3576–3587, Jul. 2012.
- [12] A. Noel, K. Cheung, and R. Schober, "Bounds on Distance Estimation via Diffusive Molecular Communication," in *IEEE Globecom*, Dec. 2014, pp. 2813–2819.
- [13] A. Ahmadzadeh, A. Noel, A. Burkovski, and R. Schober, "Amplify-and-Forward Relaying in Two-Hop Diffusion-Based Molecular Communication Networks," in *Proc. IEEE Globecom*, San Diego, Dec 2015, pp. 1–7.
- [14] X. Wang, M. Higgins, and M. Leeson, "Distance Estimation Schemes for Diffusion Based Molecular Communication Systems," *IEEE Commun. Lett.*, vol. 19, no. 3, pp. 399–402, Mar. 2015.
- [15] M. Pierobon and I. Akyildiz, "A Physical End-to-End Model for Molecular Communication in Nanonetworks," *IEEE J. Sel. Areas Commun.*, vol. 28, no. 4, pp. 602–611, May 2010.
- [16] D. Miorandi, "A Stochastic Model for Molecular Communications," *Nano Commun. Netw.*, vol. 2, no. 4, pp. 205–212, 2011.
- [17] N. Farsad, A. Eckford, and S. Hiyama, "A Markov Chain Channel Model for Active Transport Molecular Communication," *IEEE Trans. Signal. Process.*, vol. 62, no. 9, pp. 2424–2436, May 2014.
- [18] A. Noel, K. Cheung, and R. Schober, "A Unifying Model for External Noise Sources and ISI in Diffusive Molecular Communication," *IEEE J. Sel. Areas Commun.*, vol. 32, no. 12, pp. 2330–2343, Dec. 2014.
- [19] A. Bicen and I. Akyildiz, "End-to-End Propagation Noise and Memory Analysis for Molecular Communication over Microfluidic Channels," *IEEE Trans. Commun.*, vol. 62, no. 7, pp. 2432–2443, Jul. 2014.
- [20] E. Balevi and O. Akan, "A Physical Channel Model for Nanoscale Neuro-Spike Communications," *IEEE Trans. Commun.*, vol. 61, no. 3, pp. 1178–1187, Mar. 2013.
- [21] N. Farsad, N.-R. Kim, A. Eckford, and C. B. Chae, "Channel and Noise Models for Nonlinear Molecular Communication Systems," *IEEE J. Select. Areas Commun.*, vol. 32, no. 12, pp. 2392–2401, Dec. 2014.
- [22] A. Biral, D. Zordan, and A. Zanella, "Modeling, Simulation and Experimentation of Droplet-Based Microfluidic Networks," *IEEE Trans. Molecular, Biol., and Multi-Scale Commun.*, vol. 1, no. 2, pp. 122–134, Jun. 2015.
- [23] S. Crozier, D. Falconer, and S. Mahmoud, "Least Sum of Squared Errors (LSSE) Channel Estimation," *IEE Proc. F Radar Sig. Process.*, vol. 138, no. 4, pp. 371–378, Aug. 1991.
- [24] M. Ozdemir and H. Arslan, "Channel Estimation for Wireless OFDM Systems," *IEEE Commun. Surveys Tutorials*, vol. 9, no. 2, pp. 18–48, 2007.
- [25] Y. Liu, Z. Tan, H. Hu, L. Cimini, and G. Li, "Channel Estimation for OFDM," *IEEE Commun. Surveys Tutorials*, vol. 16, no. 4, pp. 1891–1908, 2014.
- [26] C. Yang, F. Yang, and Z. Wang, "Clustering-Based Adaptive Channel Estimator for Optical Fiber Communication Systems," *IEEE Photonics Technol. Lett.*, vol. 20, no. 20, pp. 1670–1672, Oct. 2008.
- [27] H. Arjmandi, A. Gohari, M. Kenari, and F. Bateni, "Diffusion-Based Nanonetworking: A New Modulation Technique and Performance Analysis," *IEEE Commun. Lett.*, vol. 17, no. 4, pp. 645–648, Apr. 2013.
- [28] R. Mosayebi, H. Arjmandi, A. Gohari, M. Nasiri-Kenari, and U. Mitra, "Receivers for Diffusion-Based Molecular Communication: Exploiting Memory and Sampling Rate," *IEEE J. Sel. Areas Commun.*, vol. 32, no. 12, pp. 2368–2380, Dec. 2014.
- [29] D. Guo, S. Shamai, and S. Verdu, "Mutual Information and Conditional Mean Estimation in Poisson Channels," *IEEE Trans. Inf. Theory*, vol. 54, no. 5, pp. 1837–1849, May 2008.
- [30] C. Gong and Z. Xu, "Channel Estimation and Signal Detection for Optical Wireless Scattering Communication with Inter-Symbol Interference," *IEEE Trans. Wireless Commun.*, vol. 14, no. 10, pp. 5326–5337, Oct. 2015.
- [31] V. Jamali, A. Ahmadzadeh, C. Jardin, C. Sticht, and R. Schober, "Channel Estimation Techniques for Diffusive Molecular Communications," in *Proc. IEEE ICC*, Kuala Lumpur, May 2016, pp. 1–7.
- [32] A. Gelman, J. B. Carlin, H. S. Stern, and D. B. Rubin, *Bayesian Data Analysis*. Taylor & Francis, 2014, vol. 2.
- [33] H. L. Van Trees, *Detection, Estimation, and Modulation Theory*. John Wiley & Sons, 2004.
- [34] M. D. Perlman, "Jensen's Inequality for a Convex Vector-Valued Function on an Infinite-Dimensional Space," *J. Multivariate Anal.*, vol. 4, no. 1, pp. 52–65, 1974.
- [35] P. H. Schonemann, "On the Formal Differentiation of Traces and Determinants," *Multivariate Behavioral Research*, vol. 20, no. 2, pp. 113–139, 1985.
- [36] S. Boyd and L. Vandenberghe, *Convex Optimization*. Cambridge, U.K.: Cambridge Univ. Press, 2004.
- [37] H. White, "A Heteroskedasticity-Consistent Covariance Matrix Estimator and a Direct Test for Heteroskedasticity," *Econometrica*, vol. 48, no. 4, pp. 817–838, 1980. [Online]. Available: <http://www.jstor.org/stable/1912934>
- [38] G. Milne, "Response of the Ordinary Least Squares Estimator (OLS) to Deterministic and Stochastic Noise," in *IEEE AFRICON*, vol. 2, Sept. 1996, pp. 1099–1104.